



Scaling FFAG for muon acceleration

JB. Lagrange, T. Planche, Y. Mori, T. Uesugi

Motivations: why scaling FFAG?

With betatron tunes that do not vary with energy, the scaling type of FFAG is:

(i) free from resonance crossing issues, **large transverse acceptances** can be achieved;

(ii) free from the issue of time-of-flight dependence on the transverse amplitude^(*). This means **no longitudinal emittance degradation** when beams with large transverse emittances are accelerated.

^(*) see S. Berg, Nucl. Instr. and Meth. A 570, p.~15, (2007).

Outline

- 🔊 Overview: 3.6 to 12.6 GeV muon ring (from T. Planche's PhD)
- 🔊 “Advanced” Scaling FFAG ingredients
- 🔊 Study of “Advanced” Scaling FFAG: experiment at KURRI
- 🔊 Applications for muons: PRISM

Outline

- Overview: 3.6 to 12.6 GeV muon ring
(from T. Planche's PhD)

- "Advanced" Scaling FFAG ingredients

- Study of "Advanced" Scaling FFAG: experiment at KURRI

- Applications for muons: PRISM

Lattice Constraints

scaling FFAG lattice:

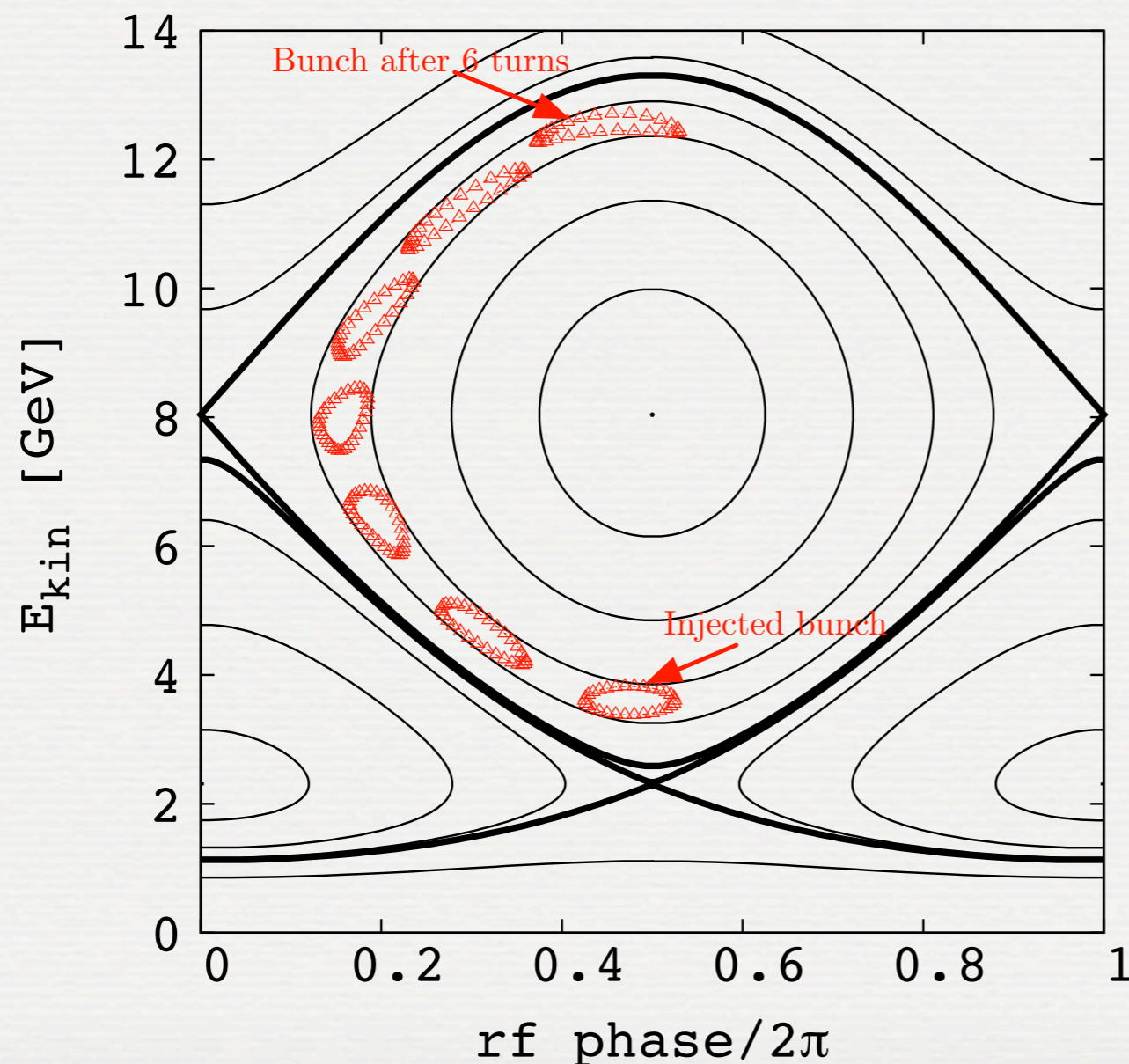
(i) with $> 30 \pi$ mm-rad of normalized transverse acceptance for both horizontal and vertical plane, and > 150 mm of normalized longitudinal acceptance,

(ii) using **200 MHz constant frequency** rf cavities

(iii) with the possibility of accelerating simultaneously μ^+ and μ^- beams.

Stationary bucket acceleration

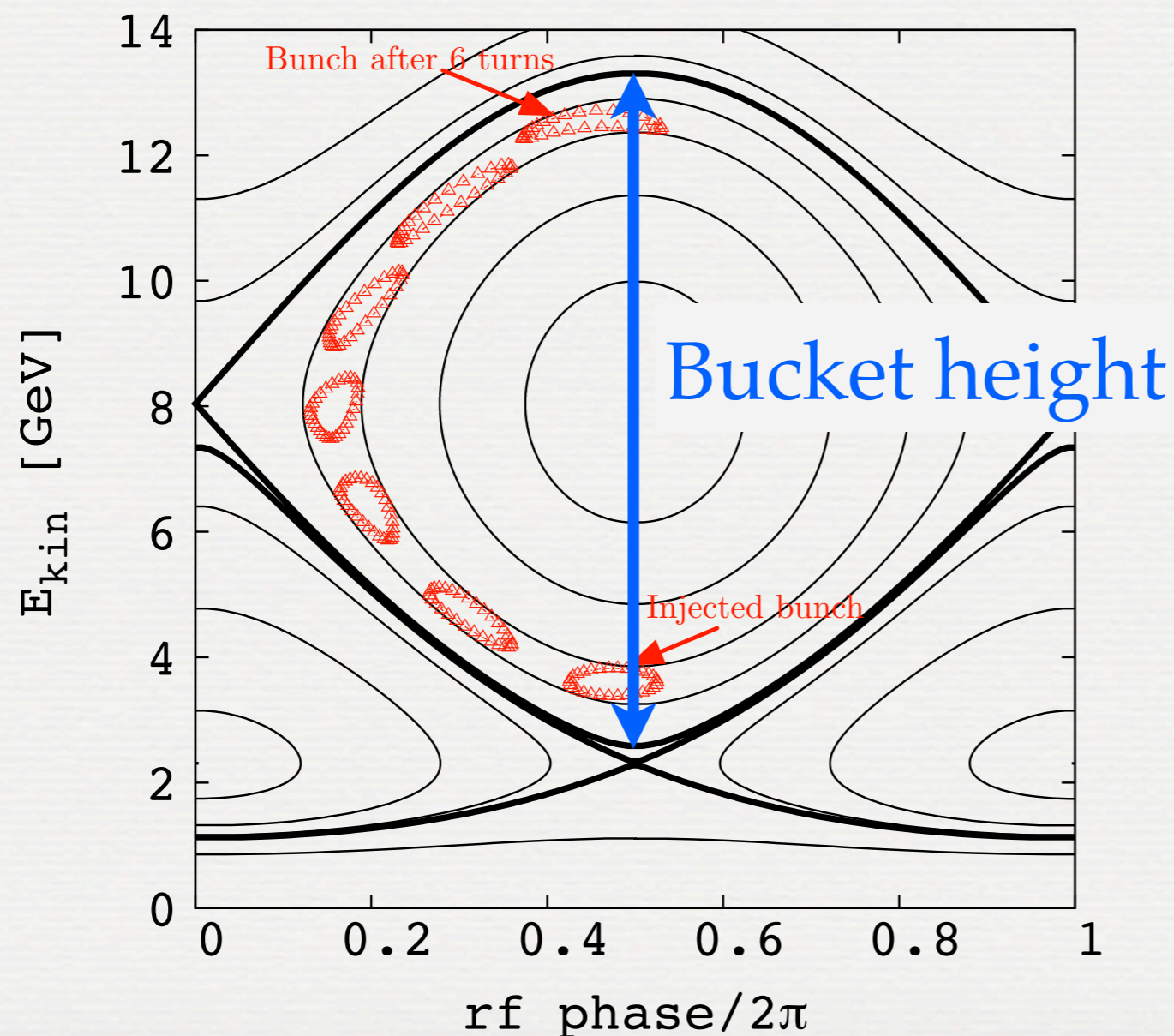
- Principle: use the synchrotron motion to accelerate beam inside a stationary rf bucket.



Longitudinal phase space showing the acceleration of a muon beam (red) inside the above transition stationary rf bucket of a scaling FFAG ring. Hamiltonian contour are shown in black.

Stationary bucket acceleration

- Principle: use the synchrotron motion to accelerate beam inside a stationary rf bucket.



Longitudinal phase space showing the acceleration of a muon beam (red) inside the above transition stationary rf bucket of a scaling FFAG ring. Hamiltonian contour are shown in black.

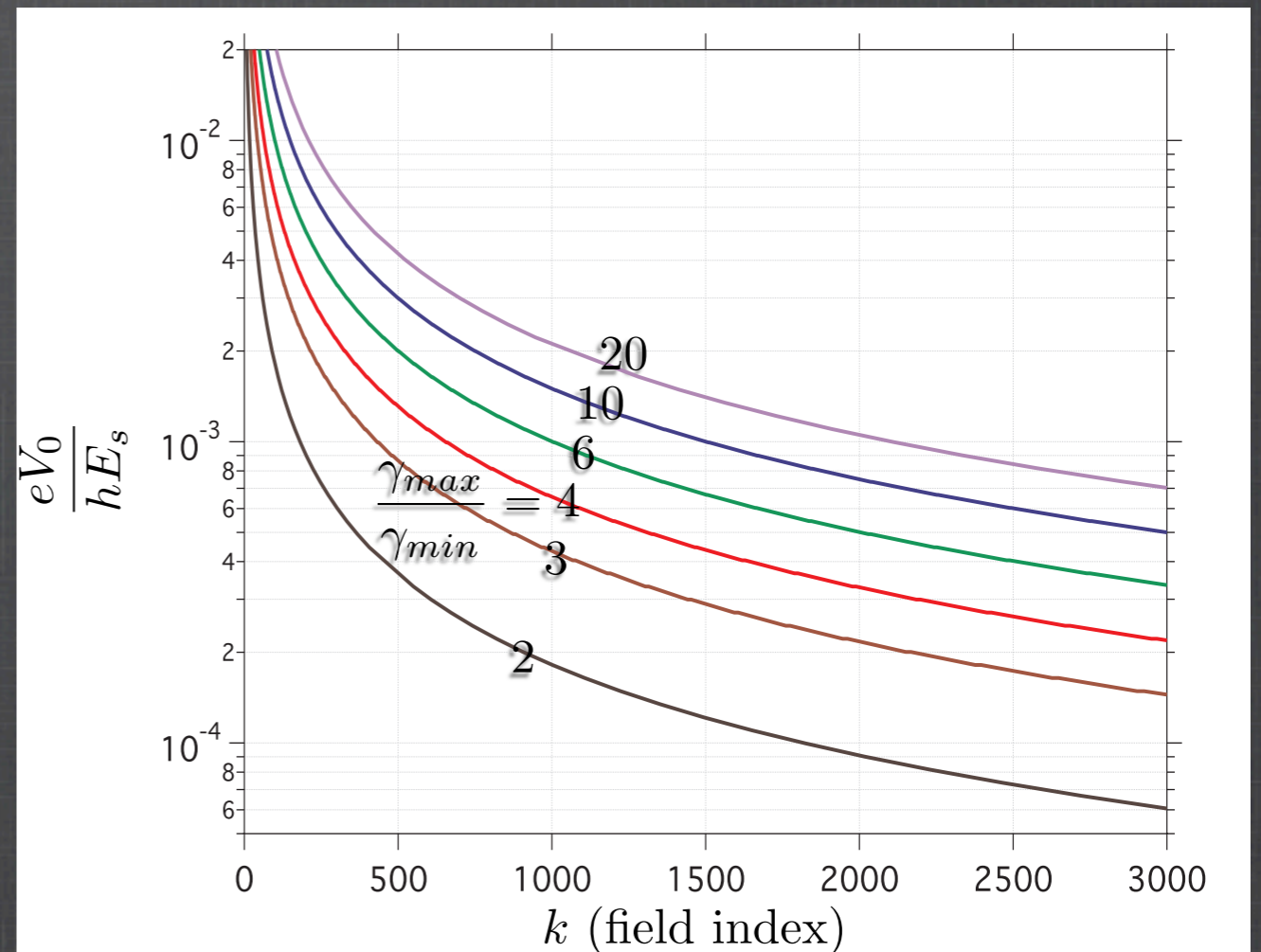
Achievable bucket height

In scaling FFAG, since the momentum compaction α is constant.

⇒ For ultra-relativistic particles, the longitudinal motion is fully determined

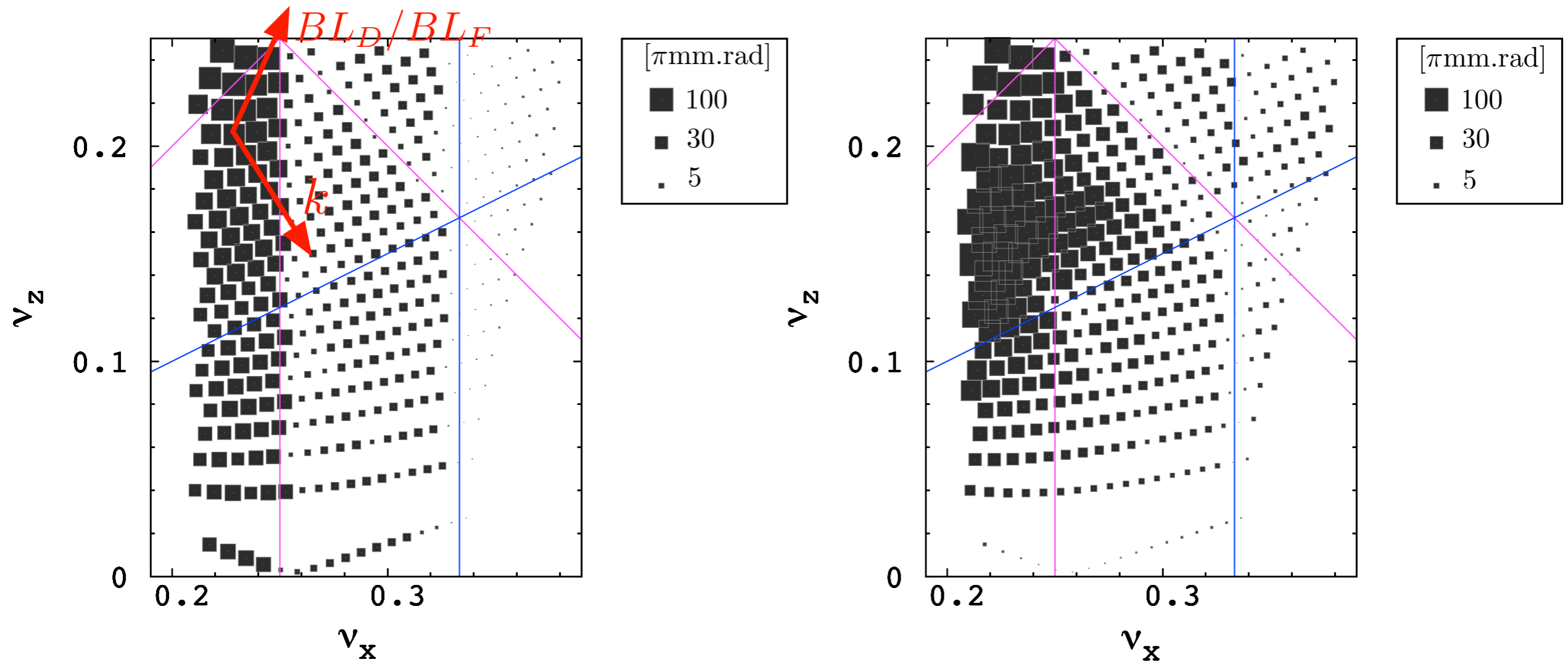
by the couple $(k, \frac{eV_0}{hE_s})$:

$$H(\phi, \gamma; \Theta) \simeq h \left[\frac{\gamma_s}{\alpha + 1} \left(\frac{\gamma}{\gamma_s} \right)^{\alpha+1} - \frac{\gamma}{\gamma_s} + \frac{1}{2\pi} \frac{eV_0}{hE_s} \cos \phi \right].$$



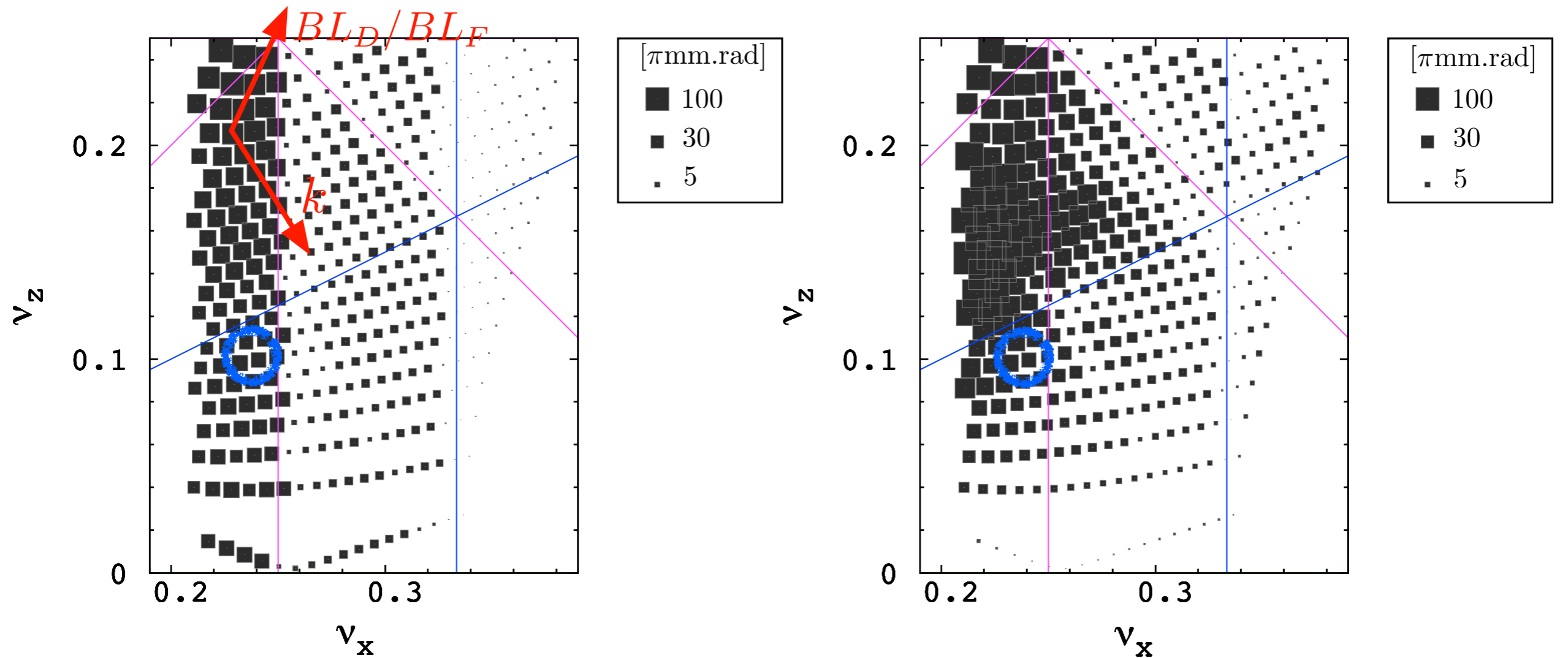
Maximum relative energy increase using acceleration inside the above-transition rf bucket of a scaling FFAG.

Transverse acceptance: choice of the working point



Horizontal (left diagram) and vertical (right diagram) acceptances scan using KUT-code. The area of each square is proportional to the normalized acceptance. Normal structure resonances lines, plotted up to the octupole, are superimposed.

Transverse acceptance: choice of the working point

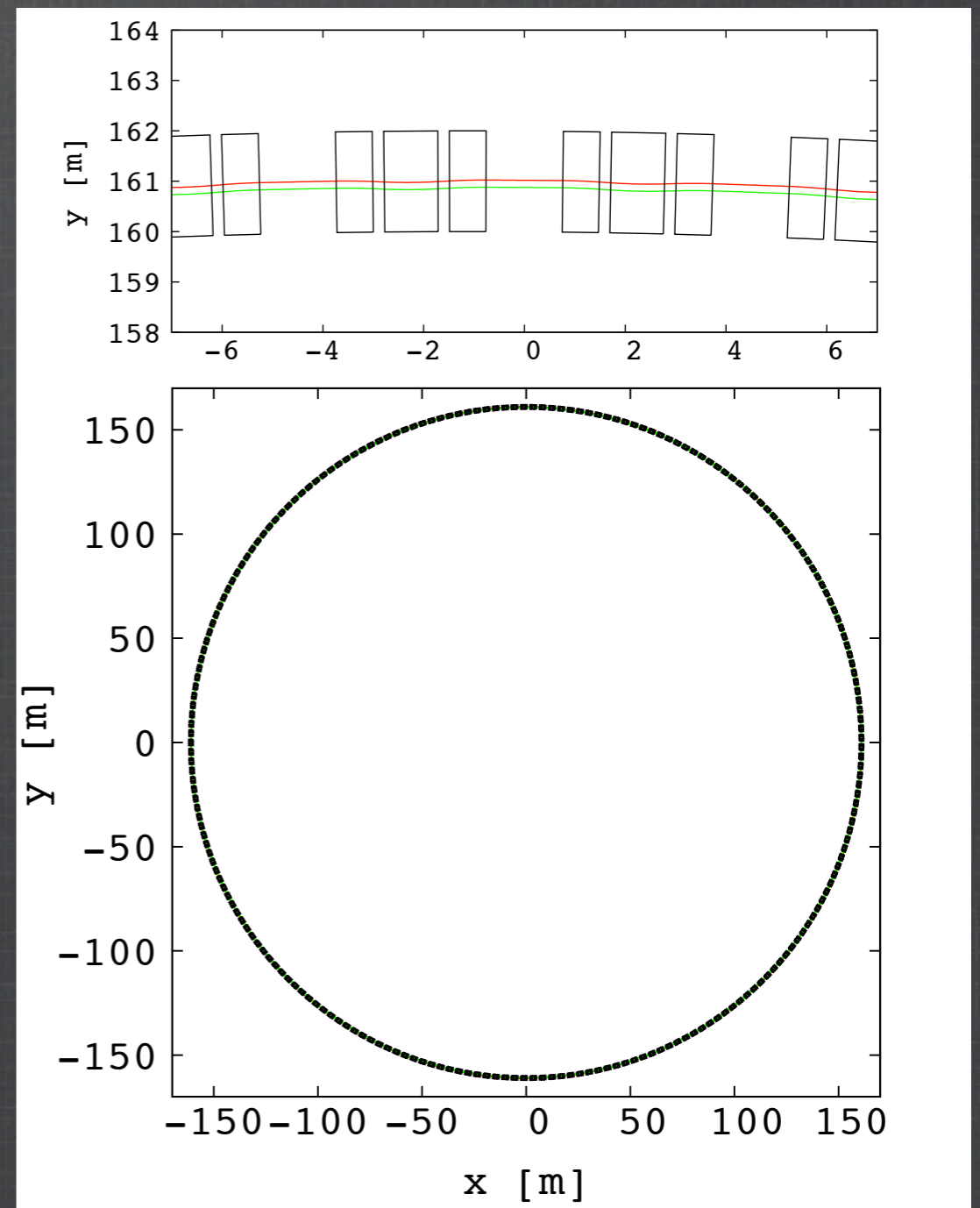


Horizontal (left diagram) and vertical (right diagram) acceptances scan using KUT-code. The area of each square is proportional to the normalized acceptance. Normal structure resonances lines, plotted up to the octupole, are superimposed.

Example of a 3.6 to 12.6 GeV muon ring

Table 1 - Scaling FFAG muon rings parameters

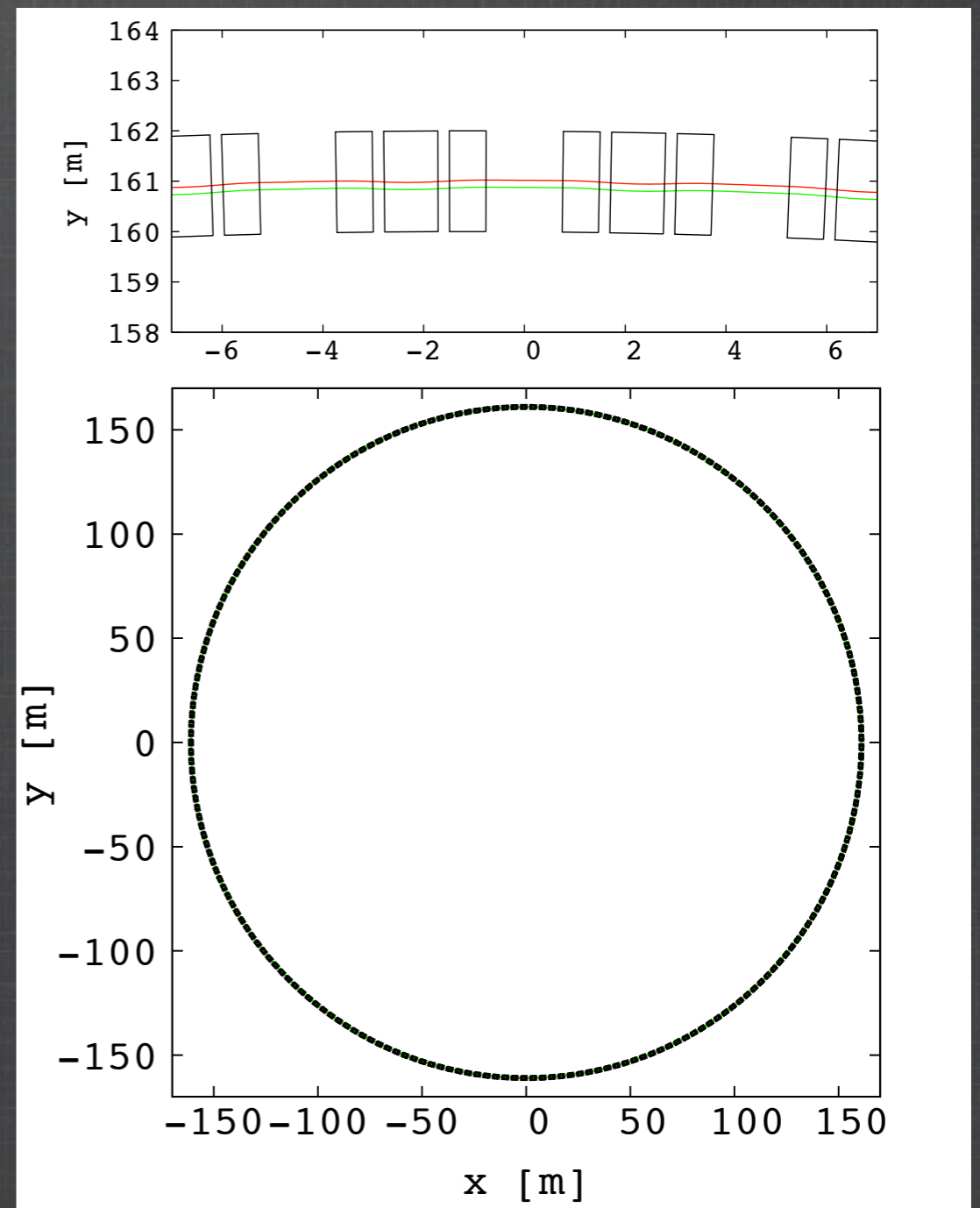
Lattice type	FDF triplet
Injection (kin) energy	3.6 GeV
Extraction energy	12.6 GeV
rf frequency	200 MHz
Mean radius	~ 161 m
Synchronous kinetic energy	8.04 GeV
Harmonic number h	675
Number of cells	225
Field index k	1390
Peak rf voltage (per turn)	1.8 GV
Number of turns	6
B_{max} (@ 12.6 GeV)	3.9 T
Drift length	~ 1.5 m
Horiz. phase adv./cell	85.86 deg.
Vert. phase adv./cell	33.81 deg.
Excursion	14.3 cm



Example of a 3.6 to 12.6 GeV muon ring

Table 1 - Scaling FFAG muon rings parameters

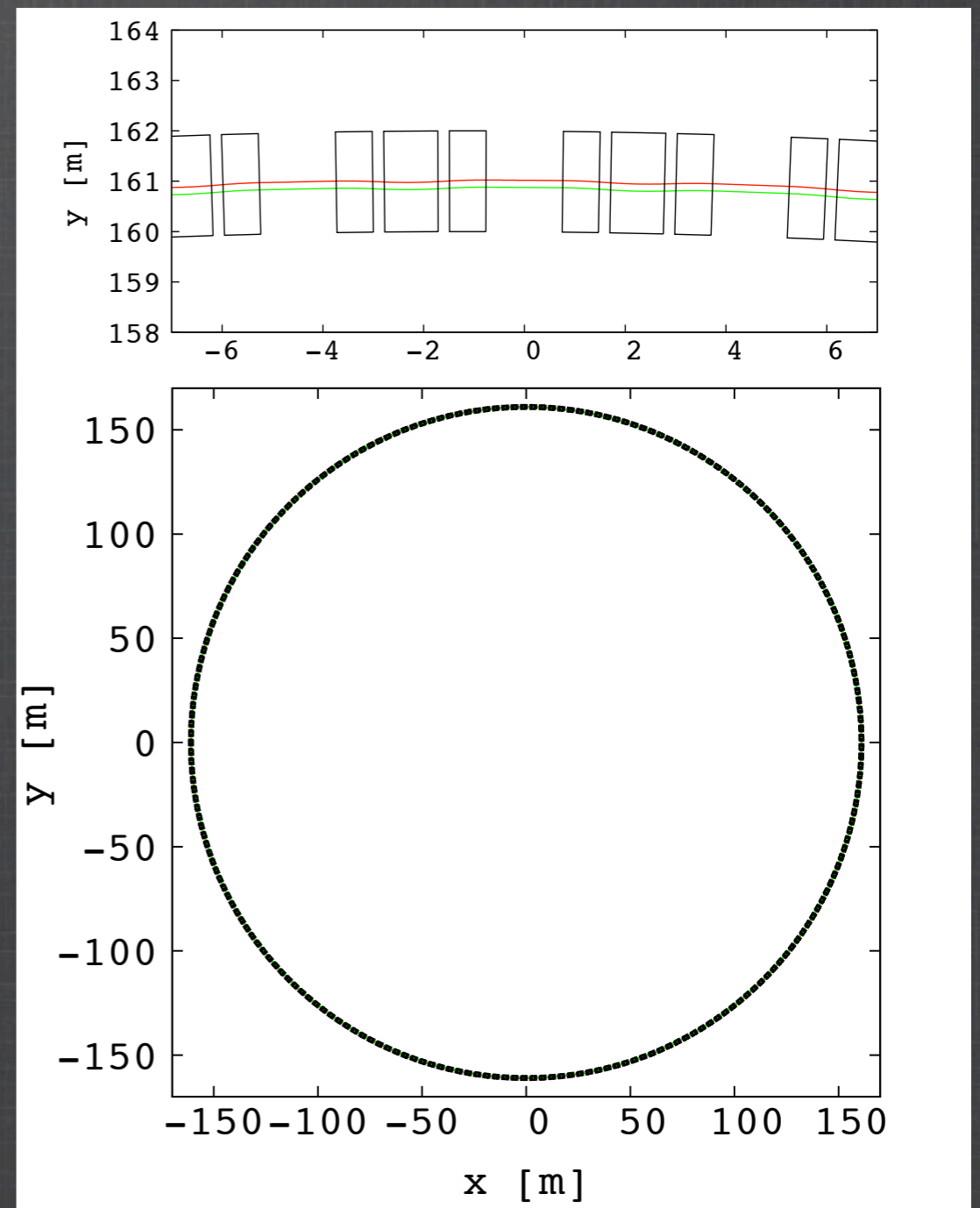
Lattice type	FDF triplet
Injection (kin) energy	3.6 GeV
Extraction energy	12.6 GeV
rf frequency	200 MHz
Mean radius	~ 101 m
Synchronous kinetic energy	8.04 GeV
Harmonic number h	675
Number of cells	225
Field index k	1390
Peak rf voltage (per turn)	1.8 GV
Number of turns	6
B_{max} (@ 12.6 GeV)	3.9 T
Drift length	~ 1.5 m
Horiz. phase adv./cell	85.86 deg.
Vert. phase adv./cell	33.81 deg.
Excursion	14.3 cm



Example of a 3.6 to 12.6 GeV muon ring

Table 1 - Scaling FFAG muon rings parameters

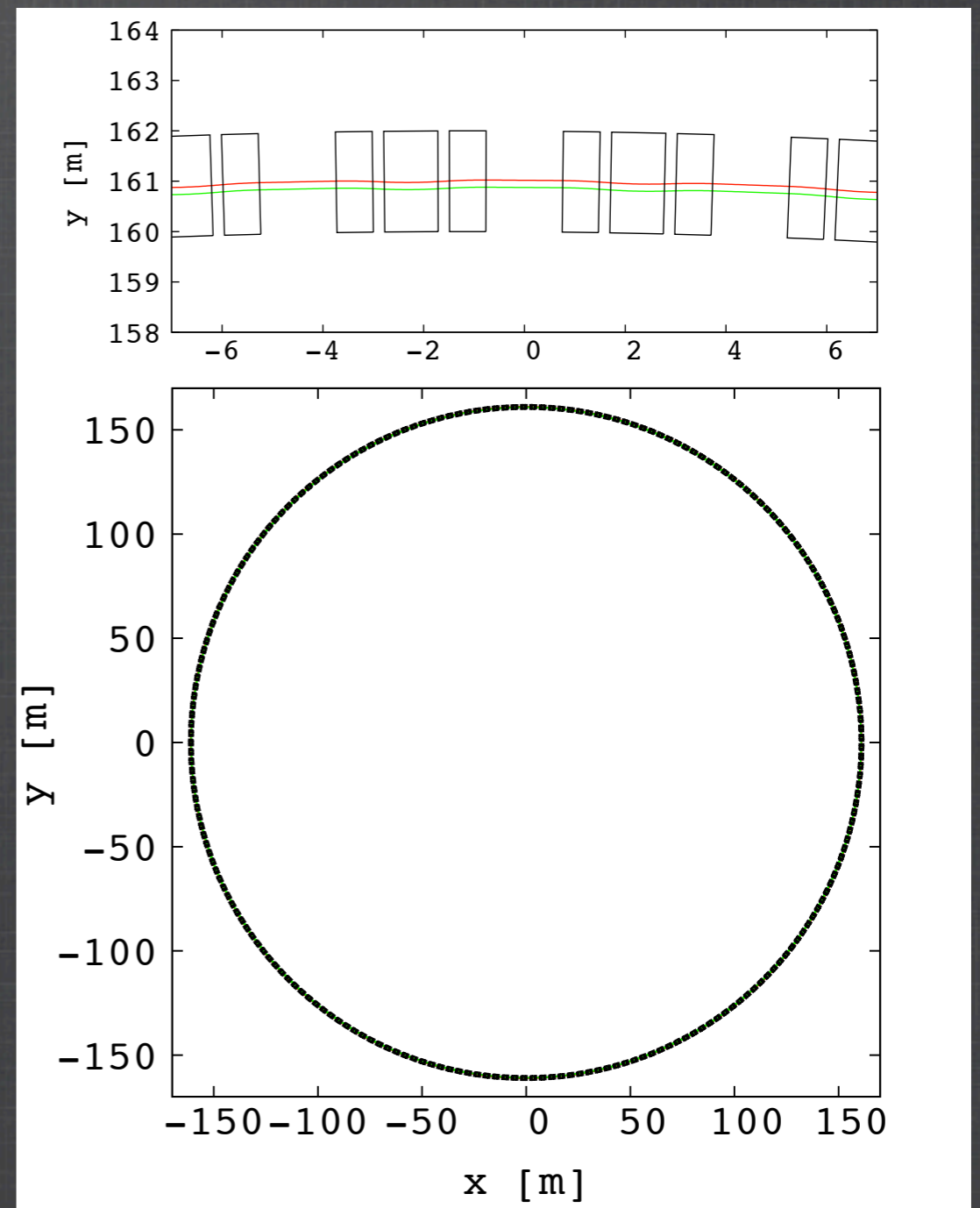
Lattice type	FDF triplet
Injection (kin) energy	3.6 GeV
Extraction energy	12.6 GeV
rf frequency	200 MHz
Mean radius	~ 161 m
Synchronous kinetic energy	8.04 GeV
Harmonic number h	675
Number of cells	225
Field index k	1390
Peak rf voltage (per turn)	1.8 GV
Number of turns	6
B_{max} (@ 12.6 GeV)	3.9 T
Drift length	~ 1.5 m
Horiz. phase adv./cell	85.86 deg.
Vert. phase adv./cell	33.81 deg.
Excursion	14.3 cm



Example of a 3.6 to 12.6 GeV muon ring

Table 1 - Scaling FFAG muon rings parameters

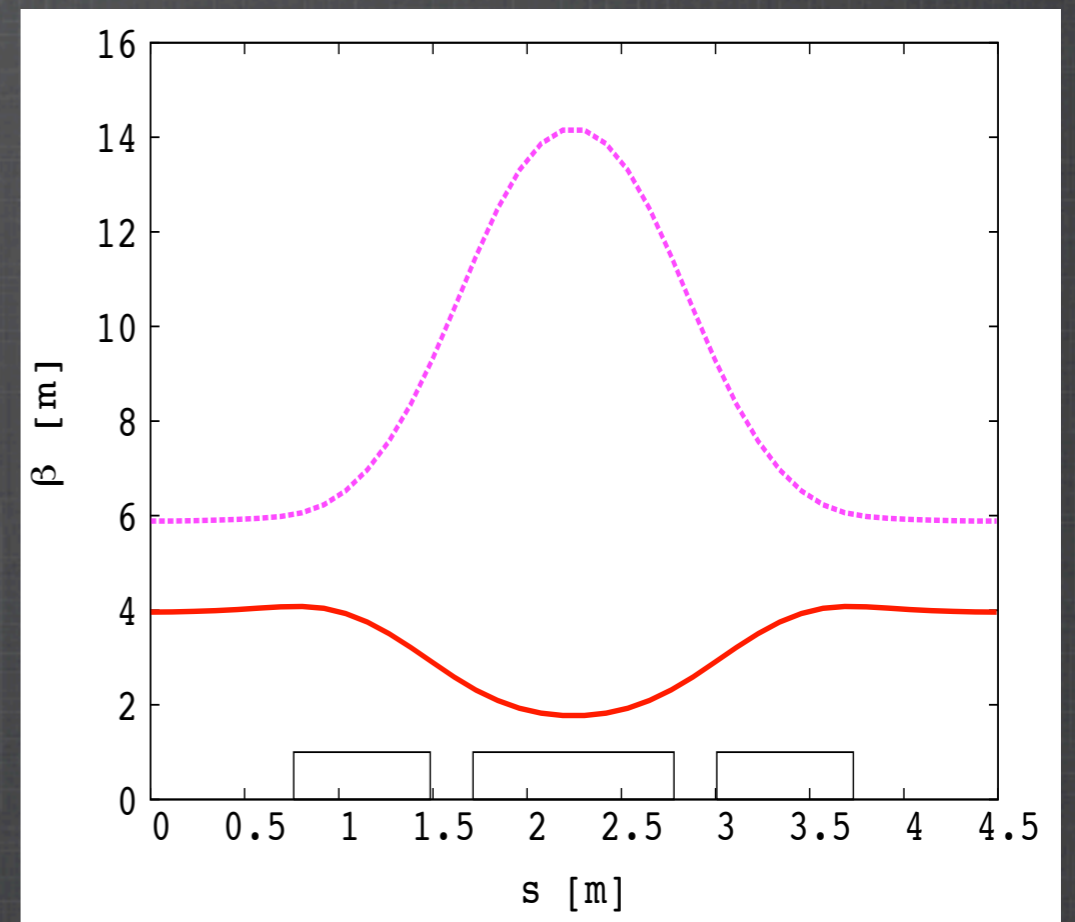
Lattice type	FDF triplet
Injection (kin) energy	3.6 GeV
Extraction energy	12.6 GeV
rf frequency	200 MHz
Mean radius	~ 161 m
Synchronous kinetic energy	8.04 GeV
Harmonic number h	675
Number of cells	225
Field index k	1390
Peak rf voltage (per turn)	1.8 GV
Number of turns	6
B_{max} (@ 12.6 GeV)	3.9 T
Drift length	~ 1.5 m
Horiz. phase adv./cell	85.86 deg.
Vert. phase adv./cell	33.81 deg.
Excursion	14.3 cm



Example of a 3.6 to 12.6 GeV muon ring

Table 1 - Scaling FFAG muon rings parameters

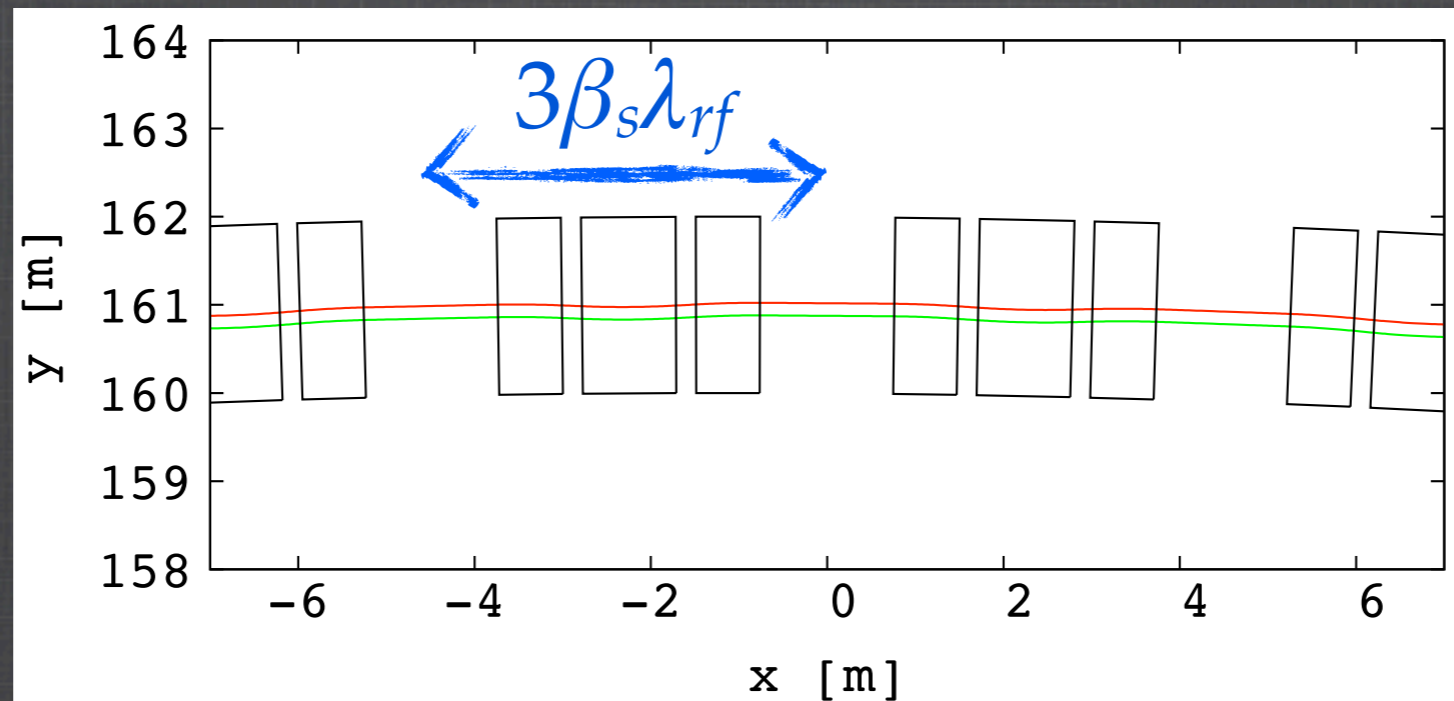
Lattice type	FDF triplet
Injection (kin) energy	3.6 GeV
Extraction energy	12.6 GeV
rf frequency	200 MHz
Mean radius	~ 161 m
Synchronous kinetic energy	8.04 GeV
Harmonic number h	675
Number of cells	225
Field index k	1390
Peak rf voltage (per turn)	1.8 GV
Number of turns	6
B_{max} (@ 12.6 GeV)	3.9 T
Drift length	~ 1.5 m
Horiz. phase adv./cell	85.86 deg.
Vert. phase adv./cell	33.81 deg.
Excursion	14.3 cm



Horizontal (red) and vertical (purple) beta function at 3.6 GeV, calculated using set-wise tracking in soft-edge field model from small amplitude motion around the closed orbit. Position of the magnets effective field boundaries are shown with rectangles.

Example of a 3.6 to 12.6 GeV muon ring

Simultaneous acceleration of μ^+ and μ^- beams:

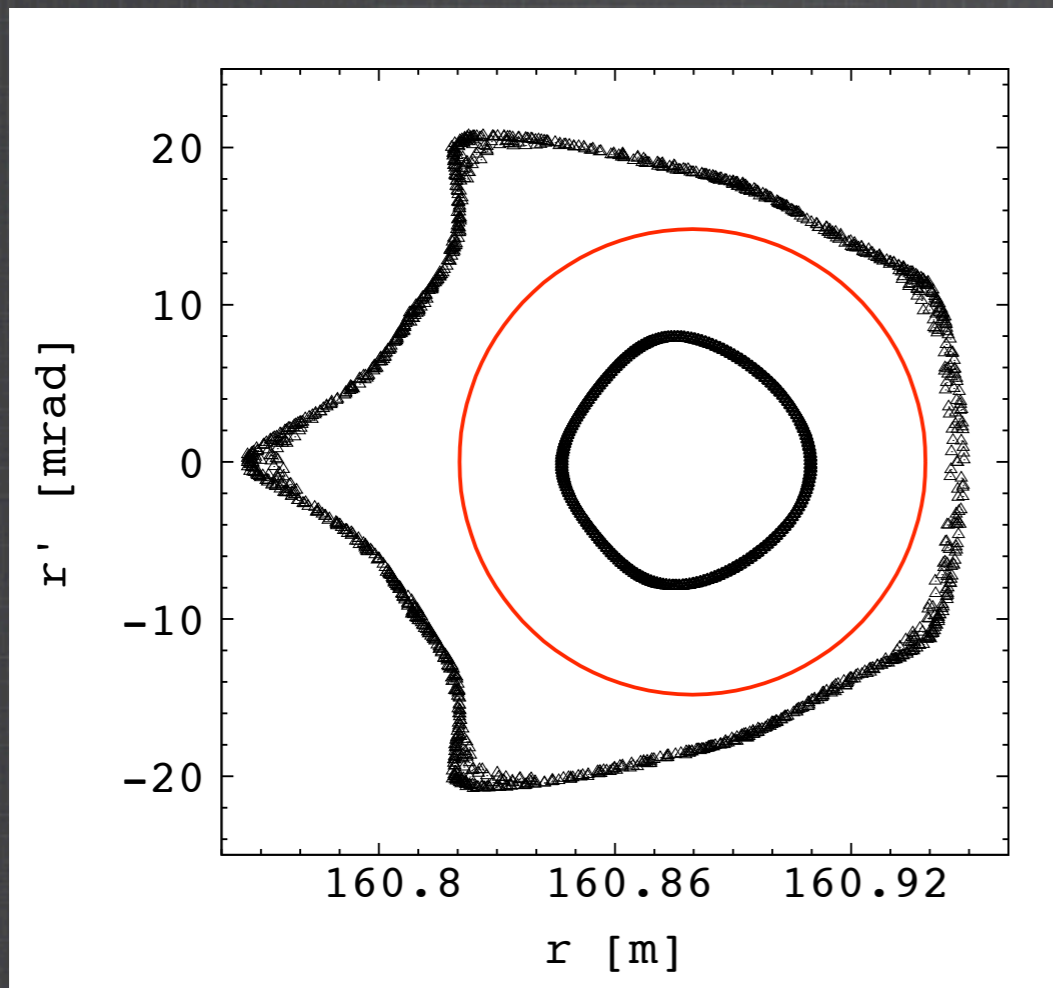


In order to allow the simultaneous acceleration of μ^+ and μ^- beams, the synchronous particle orbit length is adjusted to a multiple of $\frac{1}{2}\beta_s\lambda_{rf}$.

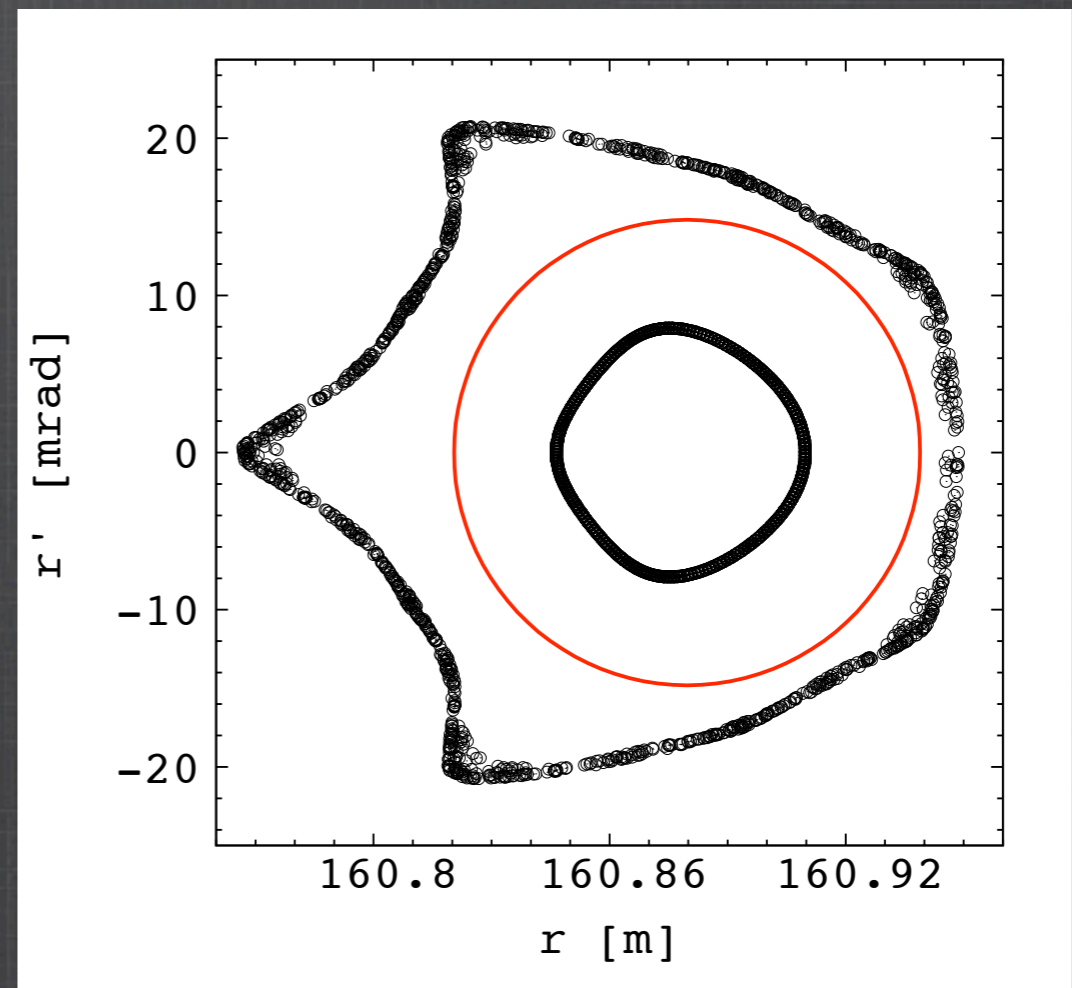
Transverse acceptance at fixed energy

Horizontal acceptance $> 30,000 \pi \cdot \text{mm} \cdot \text{mrad}$ normalized:

KUT-code



'FFAG' procedure of Zgoubi

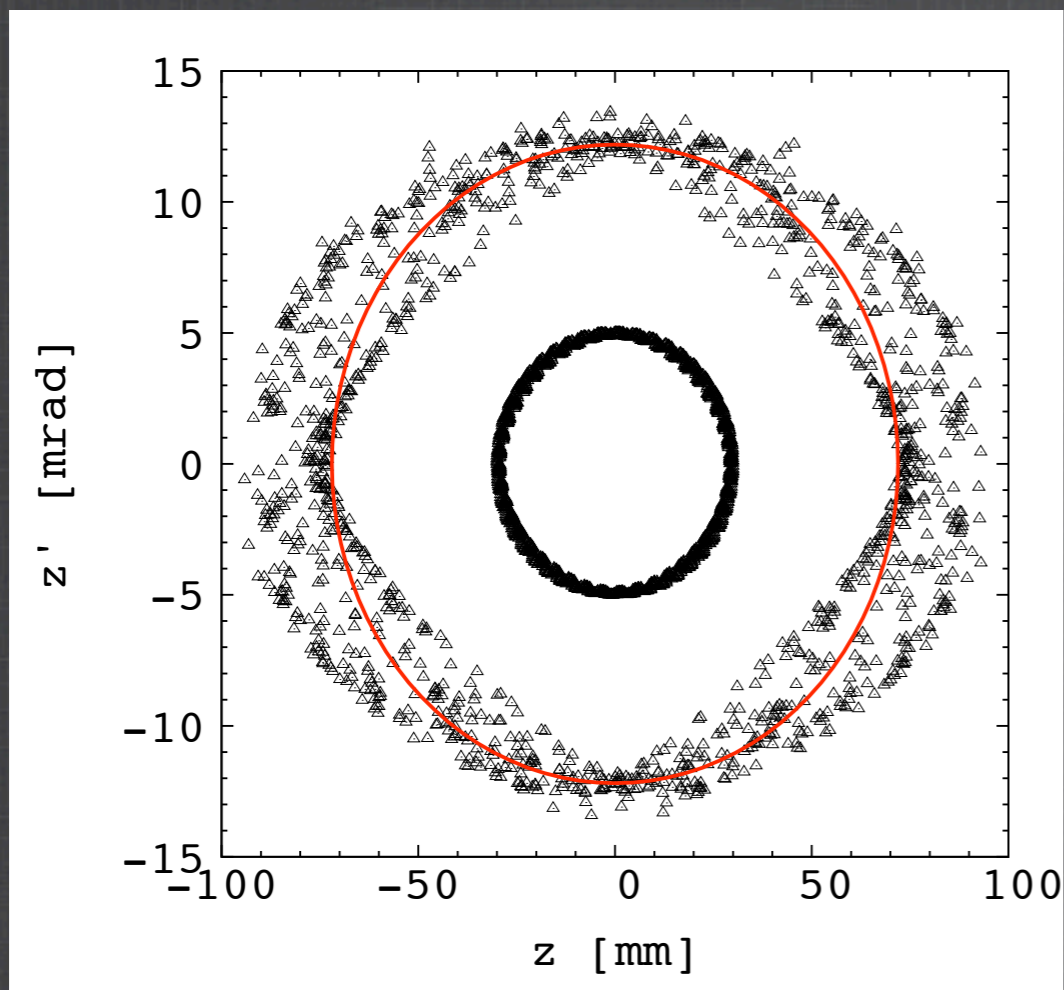


(r, r') plane showing a multi-turn tracking of 2 particles with different initial horizontal amplitudes, with an initial vertical displacement = 1 mm.

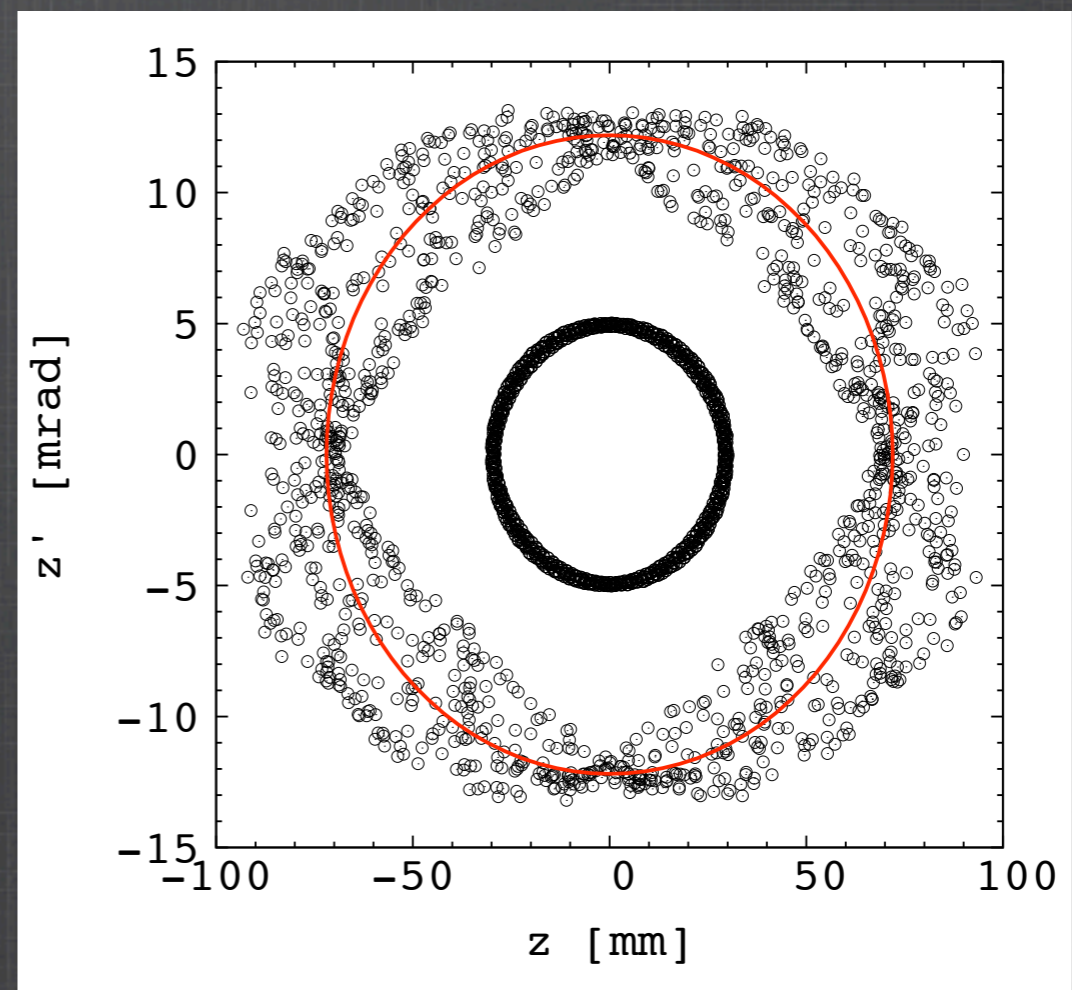
Transverse acceptance at fixed energy

Vertical acceptance $\sim 30,000 \pi \cdot \text{mm} \cdot \text{rad}$ normalized:

KUT-code



'FFAG' procedure of Zgoubi

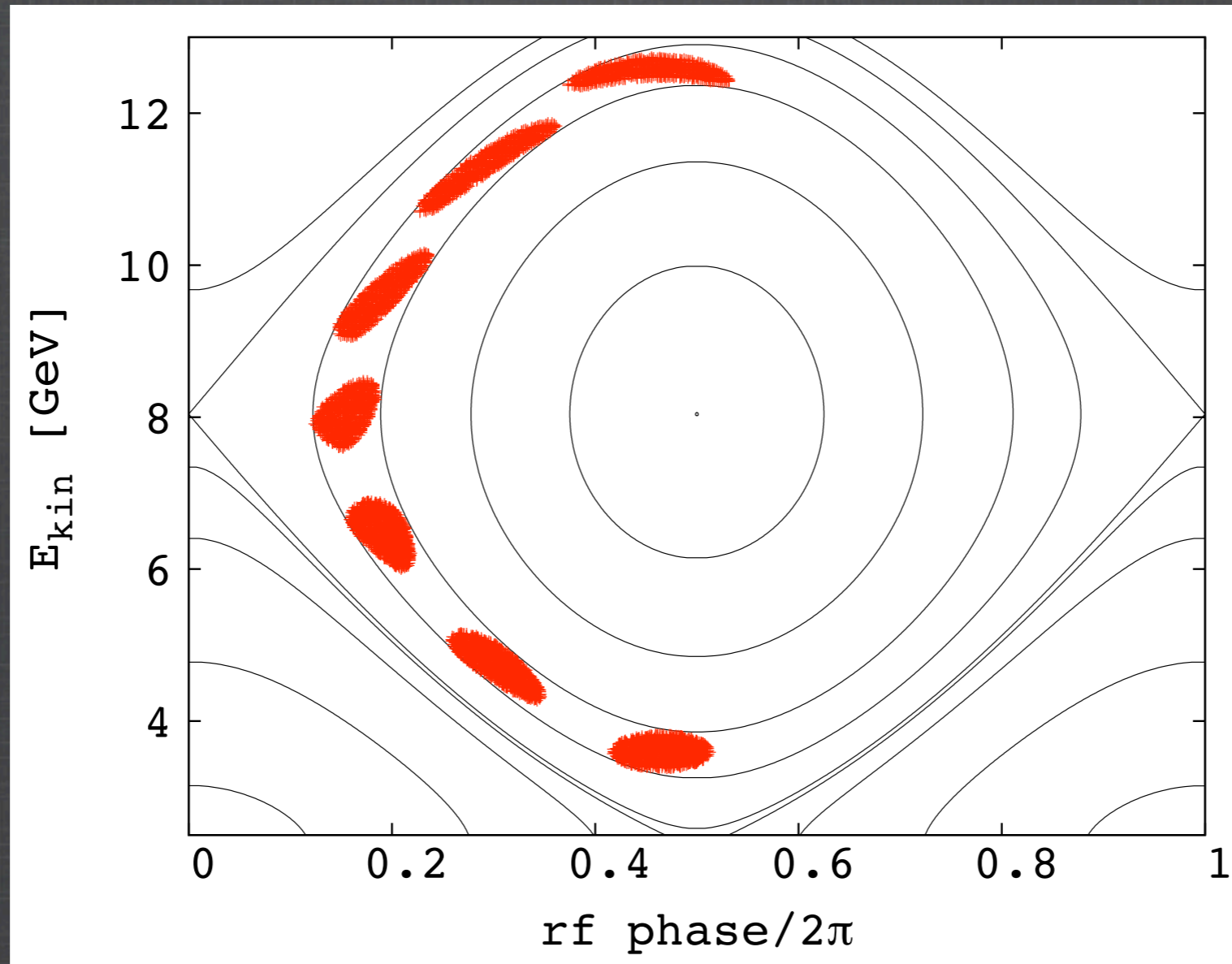


(z, z') plane showing a multi-turn tracking of 2 particles with different initial vertical amplitudes, with an initial horizontal displacement = 1 mm.

Full acceleration cycle - 6D tracking -

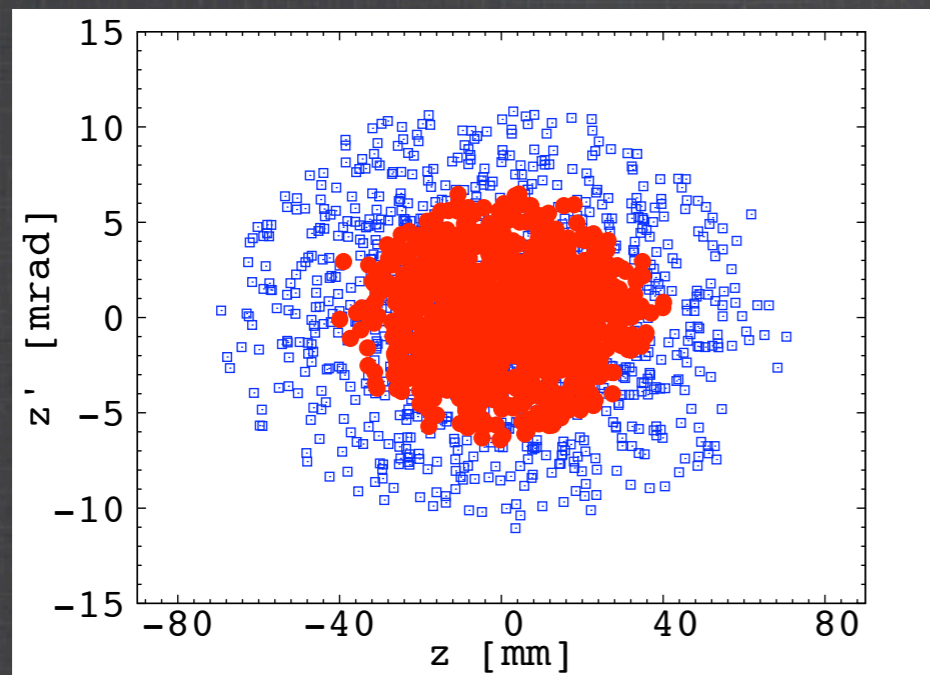
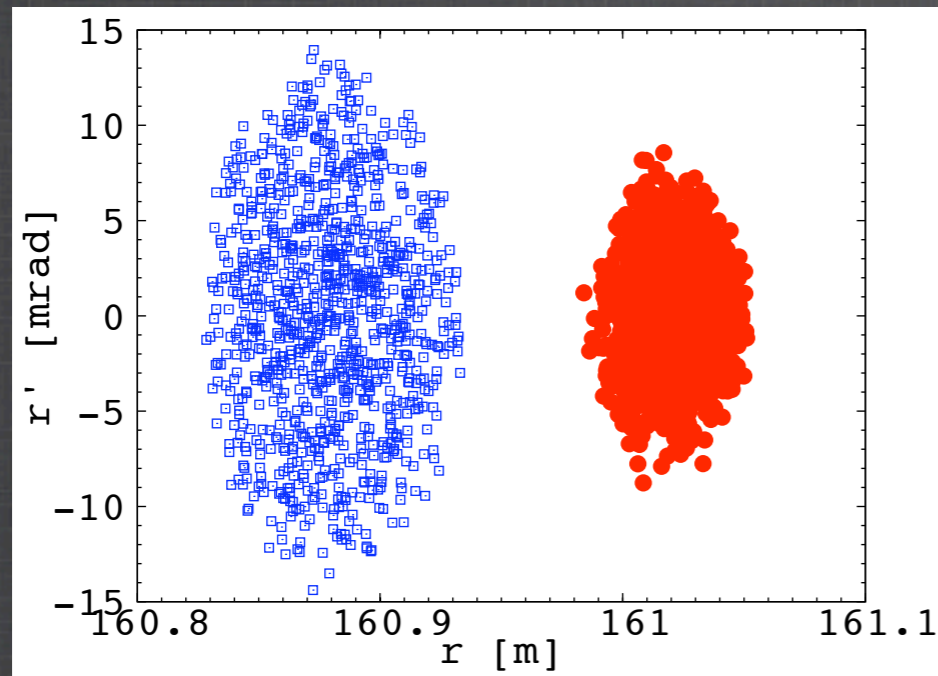
- 1000 particles are uniformly distributed inside a transverse 4D ellipsoid (Waterbag distribution).
- These particles are then independently distributed uniformly inside an ellipse in the longitudinal plane.
- Initial normalized bunch emittances are 30π .mm.rad in both horizontal and vertical planes and 150 mm in the longitudinal plane.
- RF kicks used to simulate the effect of this rf gaps distributed around the ring

6D tracking results



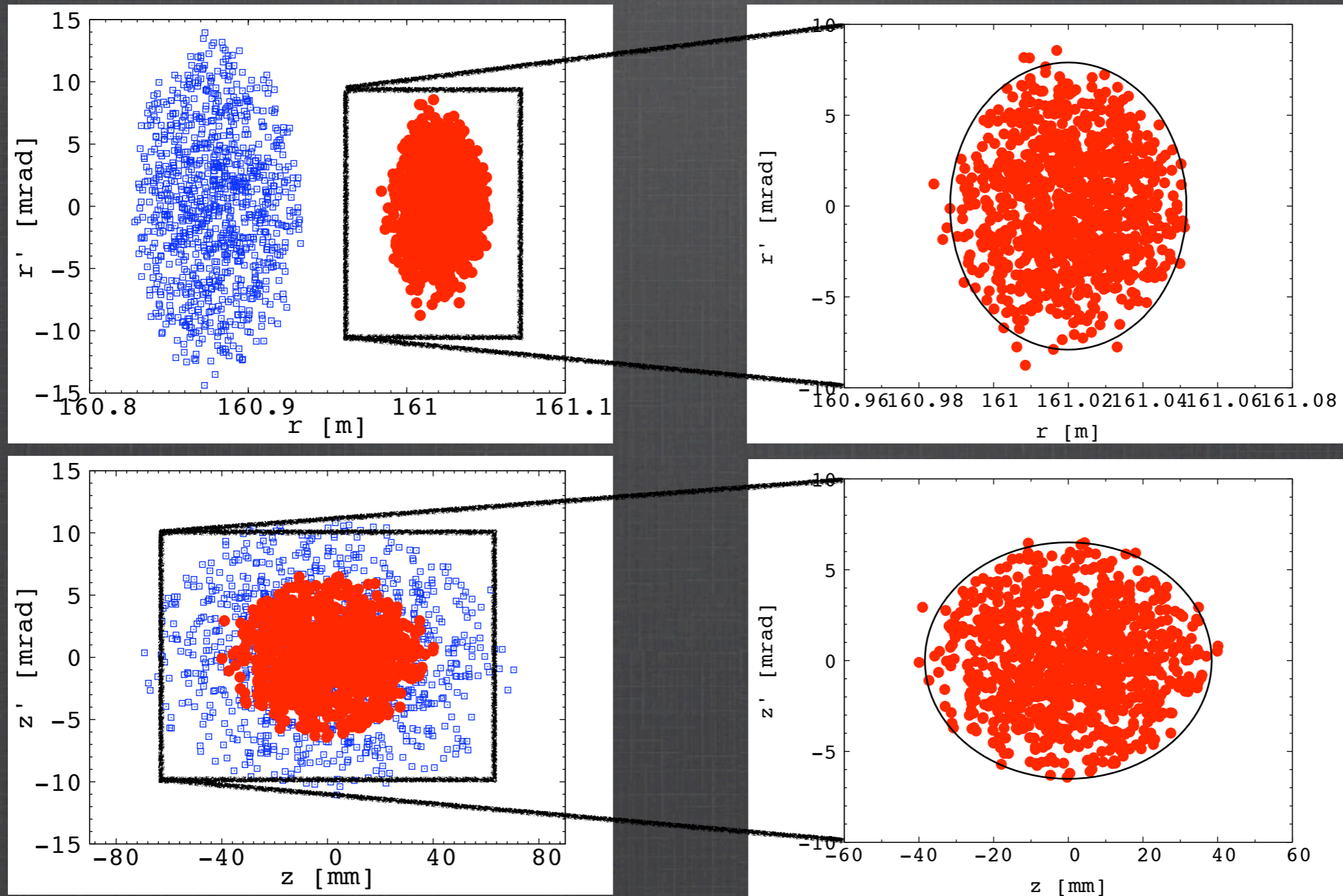
longitudinal phase space plot showing a 6-turn acceleration cycle. Hamiltonian contours are superimposed.

6D tracking results



Initial (blue) and final (red) particles distribution in the horizontal (top), and vertical (bottom) phase space.

6D tracking results



Initial (blue) and final (red) particles distribution in the horizontal (top), and vertical (bottom) phase space.

6D tracking results

- No beam loss.
- No significant transverse emittance degradation.
- No significant longitudinal emittance degradation.
- Efficient use of the rf.

Study with errors

- Direction of the translation is randomly and uniformly chosen in the 3D space. The amplitude of the displacement is chosen following a Gaussian distribution with null mean.
- 200 particles are tracked over a whole acceleration cycle (6 turns). Collimators placed in the middle of every long straight section to stop particles going at $160.7 < r < 161.1$ m, and $|z| > 90$ mm.

Overview - Summary

Overview - Summary

- World-first detailed study of stationary bucket acceleration: analytical understanding + numerical approaches.

Overview - Summary

- World-first detailed study of stationary bucket acceleration: analytical understanding + numerical approaches.
- Detailed design of a 3.6 to 12.6 GeV muon ring.

Overview - Summary

- World-first detailed study of stationary bucket acceleration: analytical understanding + numerical approaches.
- Detailed design of a 3.6 to 12.6 GeV muon ring.
- Satisfies all requirements: acceptance, RF frequency, simultaneous acceleration of μ^+ and μ^- .

Overview - Summary

- World-first detailed study of stationary bucket acceleration: analytical understanding + numerical approaches.
- Detailed design of a 3.6 to 12.6 GeV muon ring.
- Satisfies all requirements: acceptance, RF frequency, simultaneous acceleration of μ^+ and μ^- .
- Simple and robust scheme.

Overview - Summary

- World-first detailed study of stationary bucket acceleration: analytical understanding + numerical approaches.
- Detailed design of a 3.6 to 12.6 GeV muon ring.
- Satisfies all requirements: acceptance, RF frequency, simultaneous acceleration of μ^+ and μ^- .
- Simple and robust scheme.
 - ➔ Scaling FFAG can be used as an injector to the linear non-scaling FFAG.

Outline

- Overview: 3.6 to 12.6 GeV muon ring
(from T. Planche's PhD)

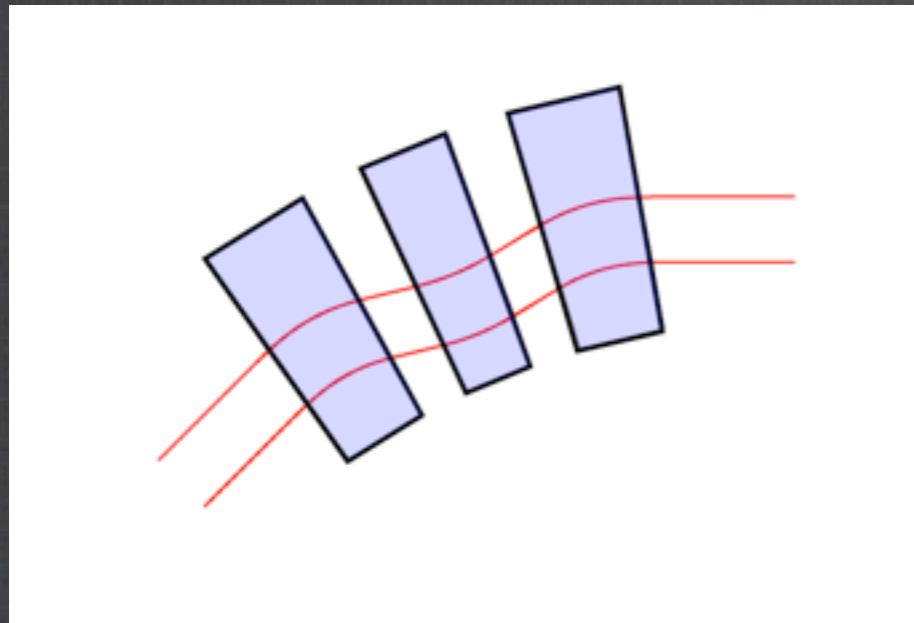
- “Advanced” Scaling FFAG ingredients

- Study of “Advanced” Scaling FFAG: experiment at KURRI

- Applications for muons: PRISM

Scaling law

Bending case



- Similarity of the closed orbits
- Invariance of the betatron oscillations

Magnetic field: $B_z = B_0 \left(\frac{r}{r_0} \right)^k$
 with $k = \frac{r}{B} \left(\frac{\partial B_z}{\partial r} \right)$

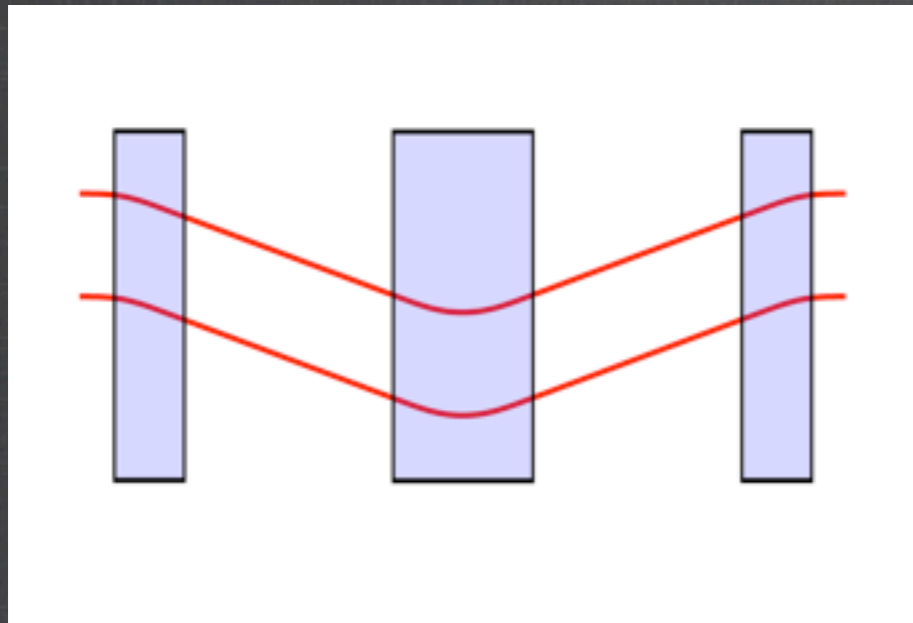
NB: In the linear approximation, $k = \frac{r}{\rho} n$

Momentum compaction factor: $\alpha = \frac{1}{k + 1}$

Dispersion function: $D(p_0) = p_0 \left(\frac{\partial r}{\partial p} \right)_{p_0} = \frac{r}{k + 1}$

Scaling law

Straight case



- Similarity of the closed orbits
- Invariance of the betatron oscillations

Magnetic field: $B_z = B_0 e^{m(x-x_0)}$

$$\text{with } m = \frac{1}{B} \left(\frac{\partial B_z}{\partial x} \right)$$

NB: In the linear approximation, $m = \frac{n}{\rho}$

Momentum compaction factor: $\alpha = 0$

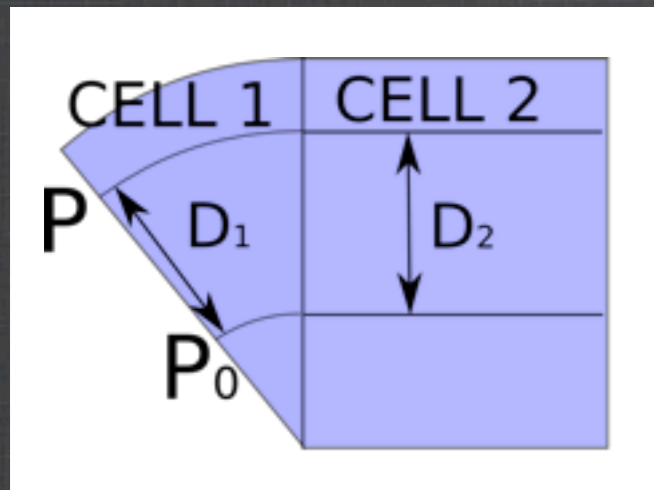
Dispersion function: $D(p_0) = p_0 \left(\frac{\partial x}{\partial p} \right)_{p_0} = \frac{1}{m}$

$$\text{Linear approx.: } \lim_{r_0 \rightarrow \infty} \left(\frac{r}{r_0} \right)^k = \lim_{r_0 \rightarrow \infty} \left[\left(1 + \frac{x}{r_0} \right)^{\frac{r_0}{x}} \right]^{\frac{x}{r_0} k} = \left[\lim_{r_0 \rightarrow \infty} \left(1 + \frac{x}{r_0} \right)^{\frac{r_0}{x}} \right]^{\frac{n}{\rho} x} = e^{\frac{n}{\rho} x} = e^{mx}$$

Insertions

Matching of different scaling FFAG cells

1) Matching of the closed/reference orbits



- Matching of a special momentum P_0 .
- Matching to the first order in $\Delta R/R_0$ by matching of the dispersion of the different cells.

2) Matching of the periodic linear parameters

As much as possible (the more the better)

Often difficult \longrightarrow π -phase advance for one of the cell(s)

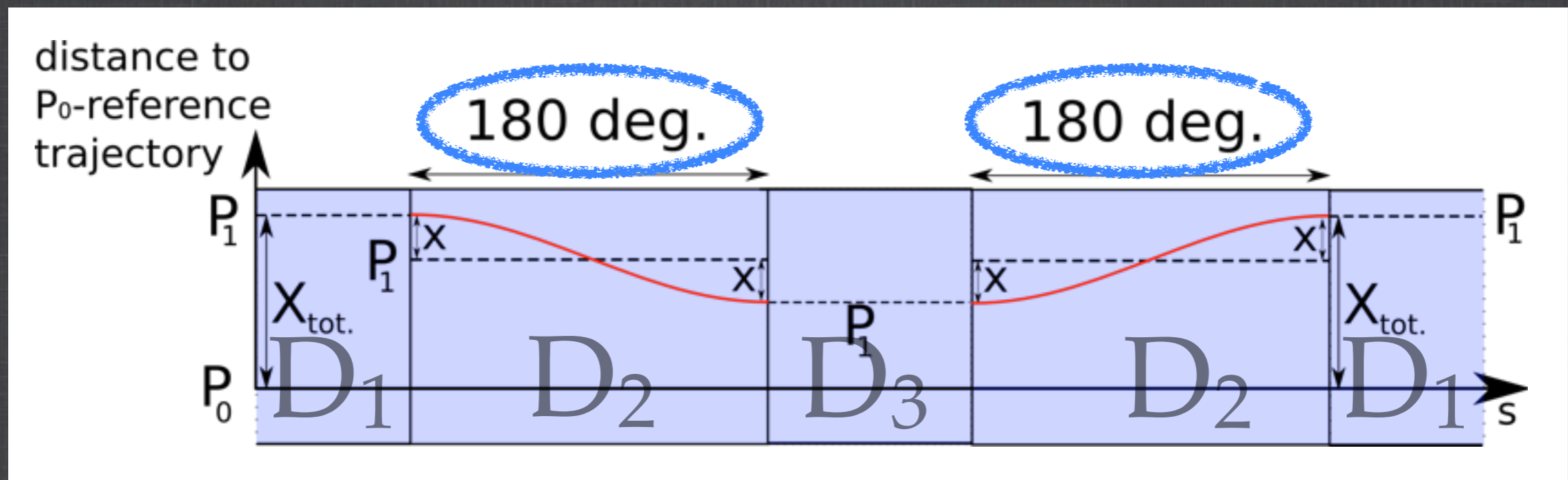
Insertions

Dispersion suppressor principle

Use of 3 different scaling FFAG cells

a) Matching of a special momentum P_0 .

b) Matching of periodic dispersions such as $D_2 = \frac{D_1 + D_3}{2}$



Zero-chromatic system as long as amplitude detuning can be neglected.

Outline

- Overview: 3.6 to 12.6 GeV muon ring
(from T. Planche's PhD)

- "Advanced" Scaling FFAG ingredients

- Study of "Advanced" Scaling FFAG: experiment at KURRI

- Applications for muons: PRISM

Study of Advanced Scaling FFAG

In Kyoto University, an experiment is planned to be conducted in order to study these new tools.

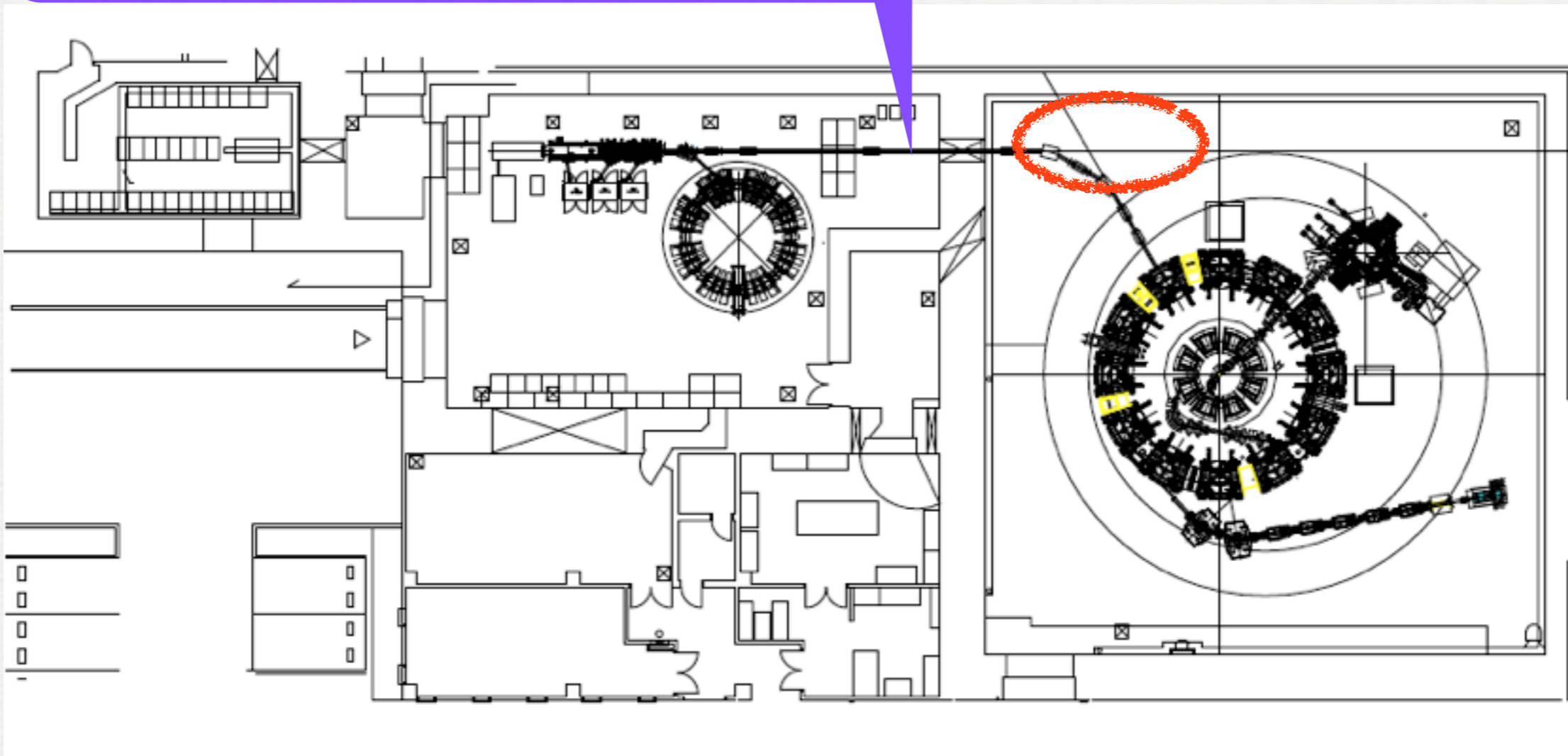
2 goals for this experiment:

- Verify the straight field law,
- Verify and study the dispersion suppressor principle.

Experiment

Layout of the experiment

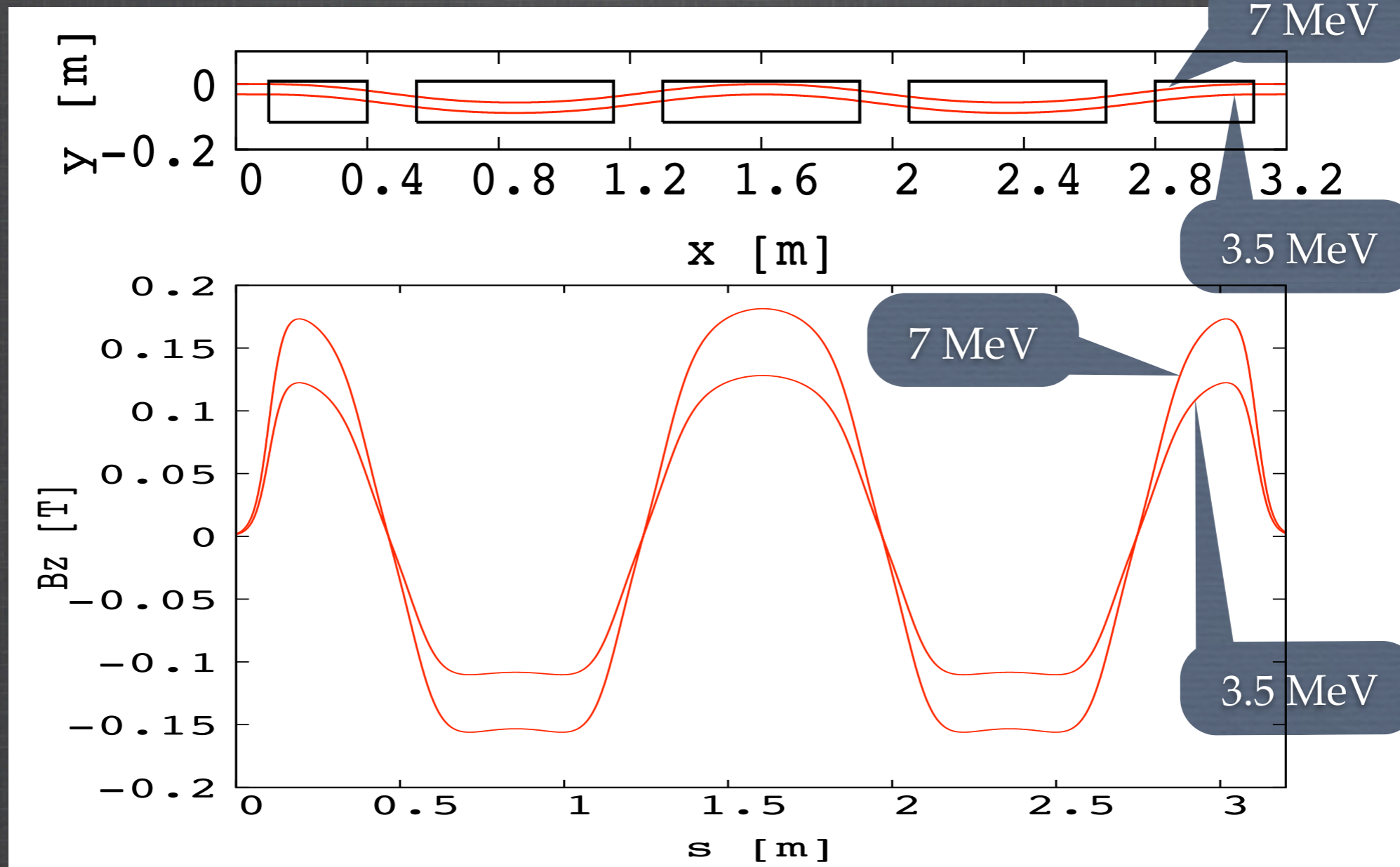
H⁻ linac injection beam line



Use of 2 energies: 3.5 MeV and 7 MeV.

Experiment

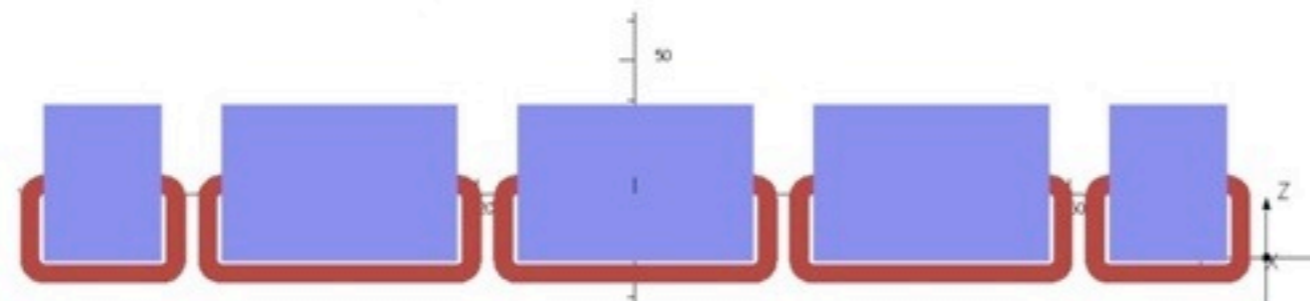
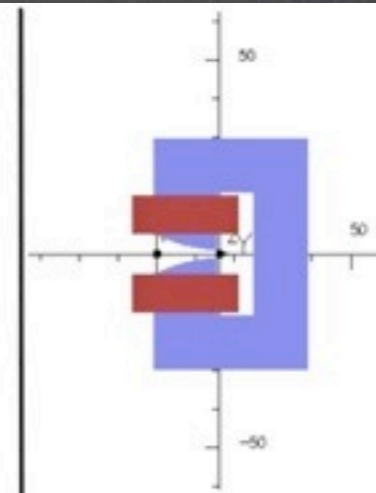
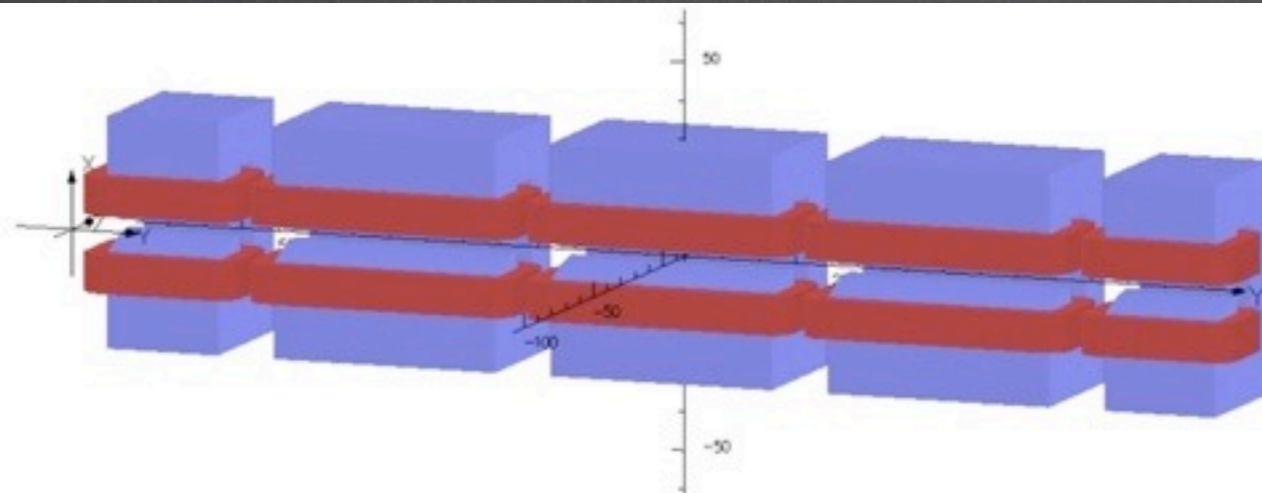
Straight field law



Use of steering magnets for the shifts of the orbits

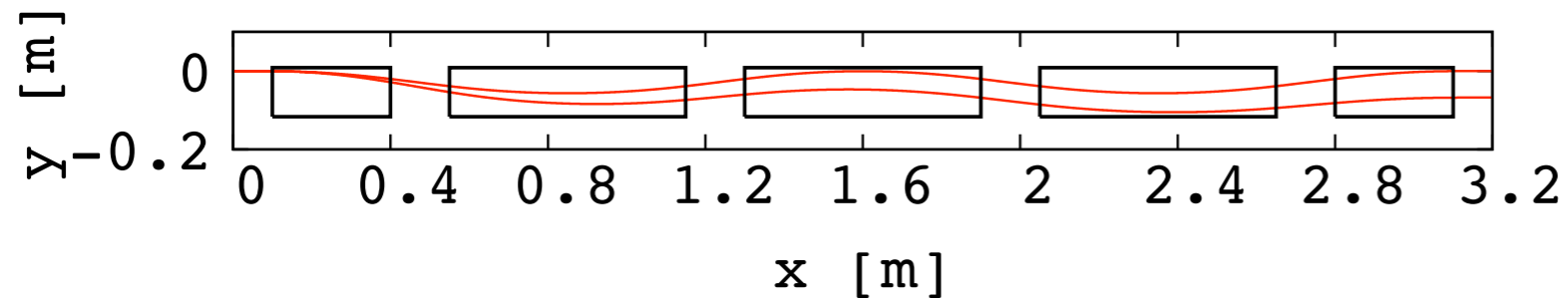
Experiment

Dispersion suppressor and magnets



FI D F2 D FI

Schematic view of scaling FFAG line and dispersion suppressor prototype



Outline

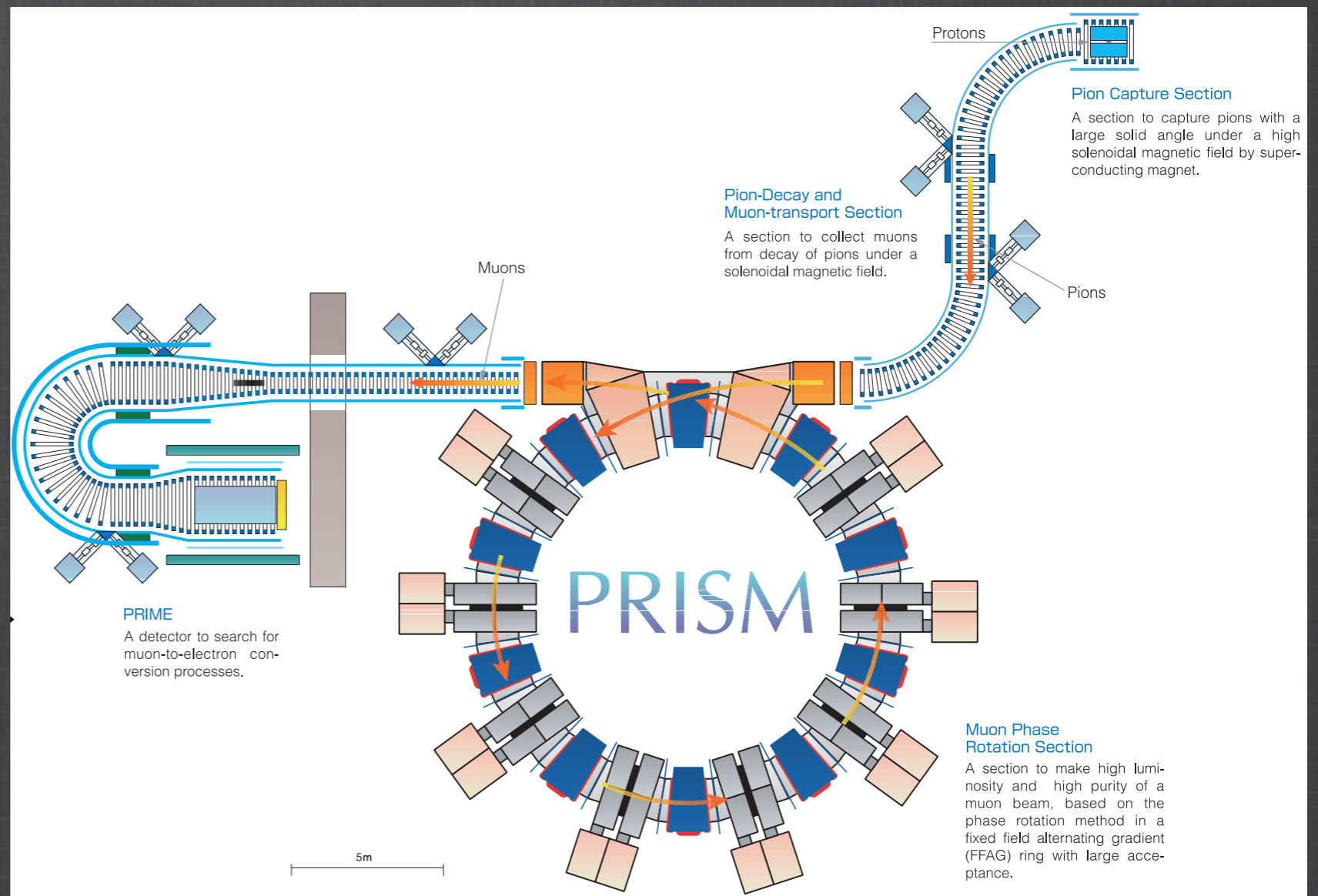
- 📌 Overview: 3.6 to 12.6 GeV muon ring (from T. Planche's PhD)
- 📌 "Advanced" Scaling FFAG ingredients
- 📌 Study of "Advanced" Scaling FFAG: experiment at KURRI
- 📌 Applications for muons: PRISM

Applications

PRISM project

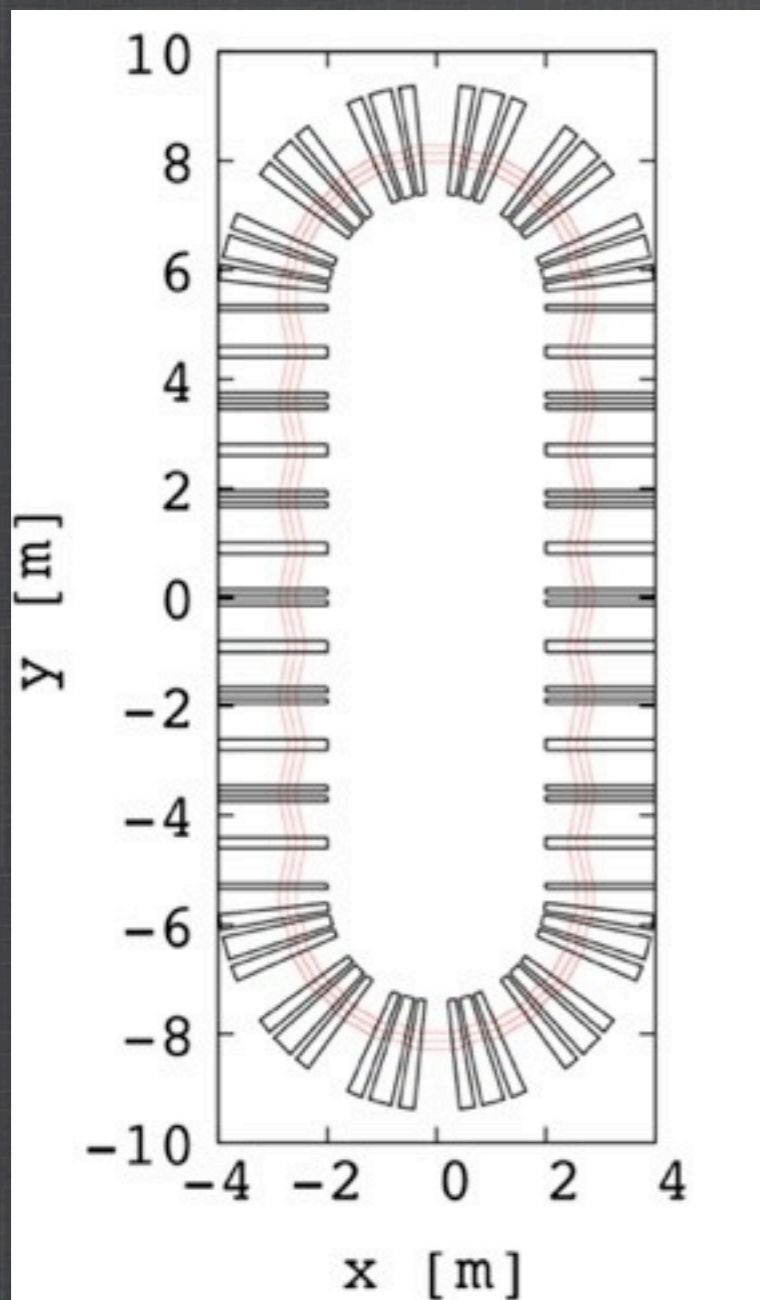
Muon phase rotator (at Osaka University)

- Momentum acceptance:
 $68\text{MeV}/c \pm 20\%$
- Transverse acceptance:
 - hor.: $30\,000\pi$ mm.mrad
 - vert.: $3\,000\pi$ mm.mrad



Applications

Race-track scaling FFAG PRISM



Bending cell FDF triplet

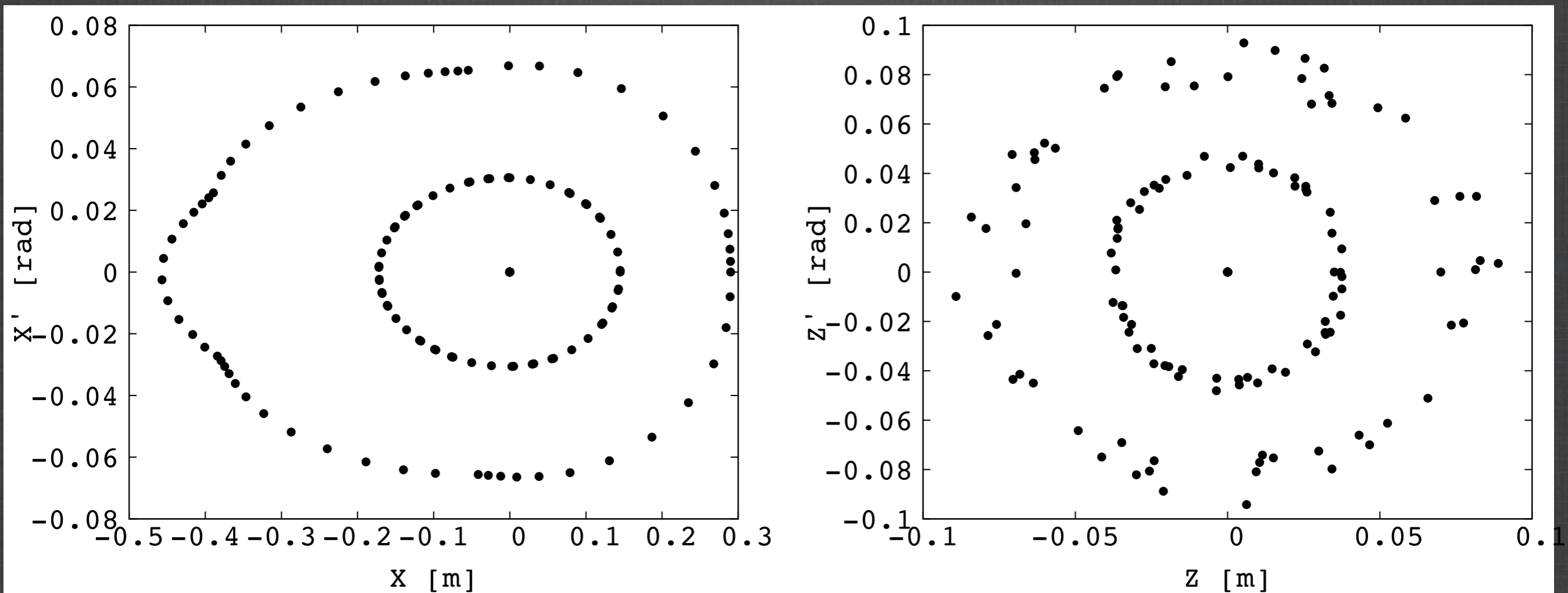
k -value	2.55
Average radius	2.7 m
Phase advances:	
Horizontal μ_x	60 deg.
Vertical μ_z	90 deg.
Dispersion	0.8 m

Straight cell

m -value	1.3 m^{-1}
Length	1.8 m
Phase advances:	
Horizontal μ_x	27 deg.
Vertical μ_z	94 deg.
Dispersion	0.8 m

Applications

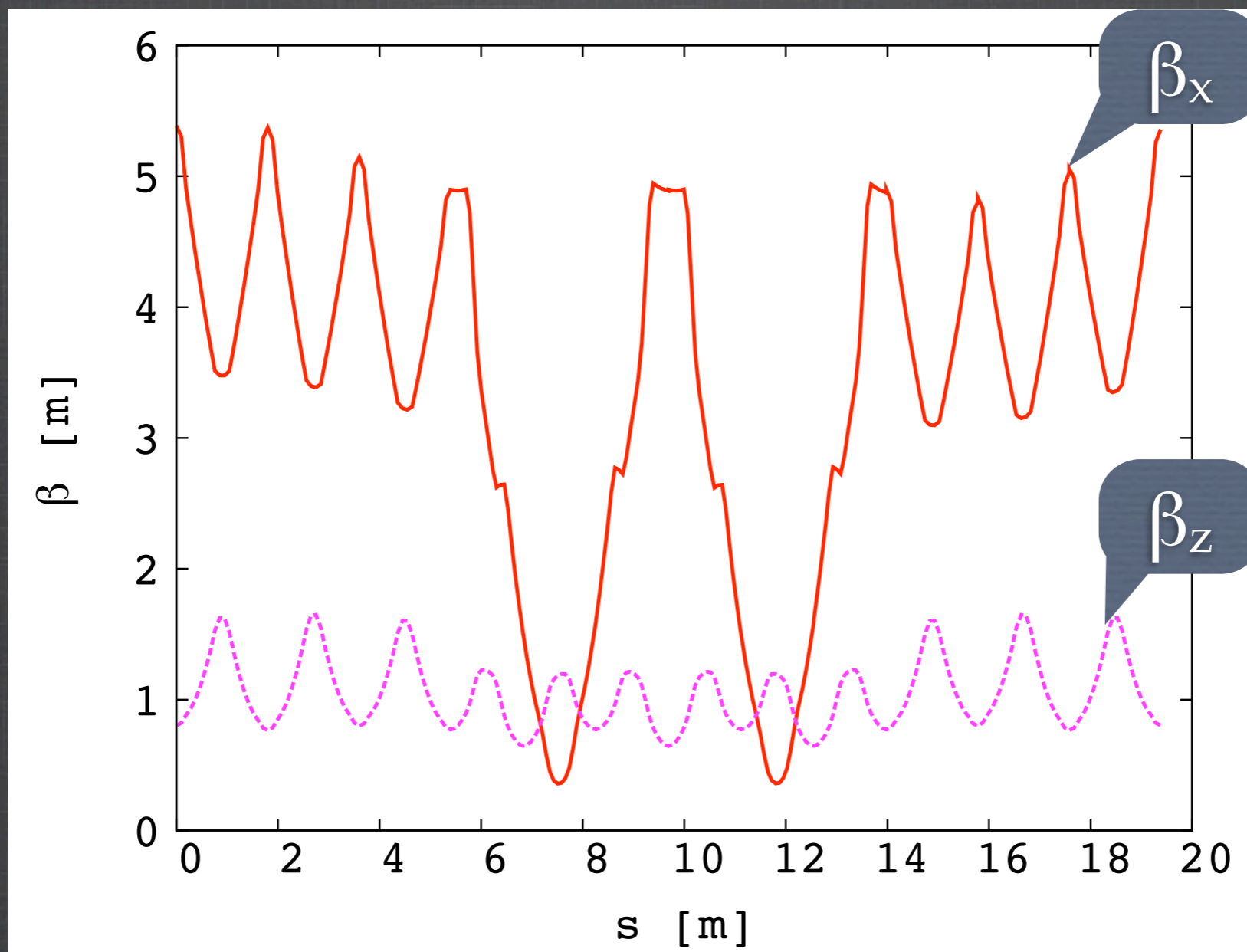
Acceptances of race-track PRISM



Horizontal (left) and vertical (right) acceptance of the ring over 30 turns
Far collimators identify lost particles

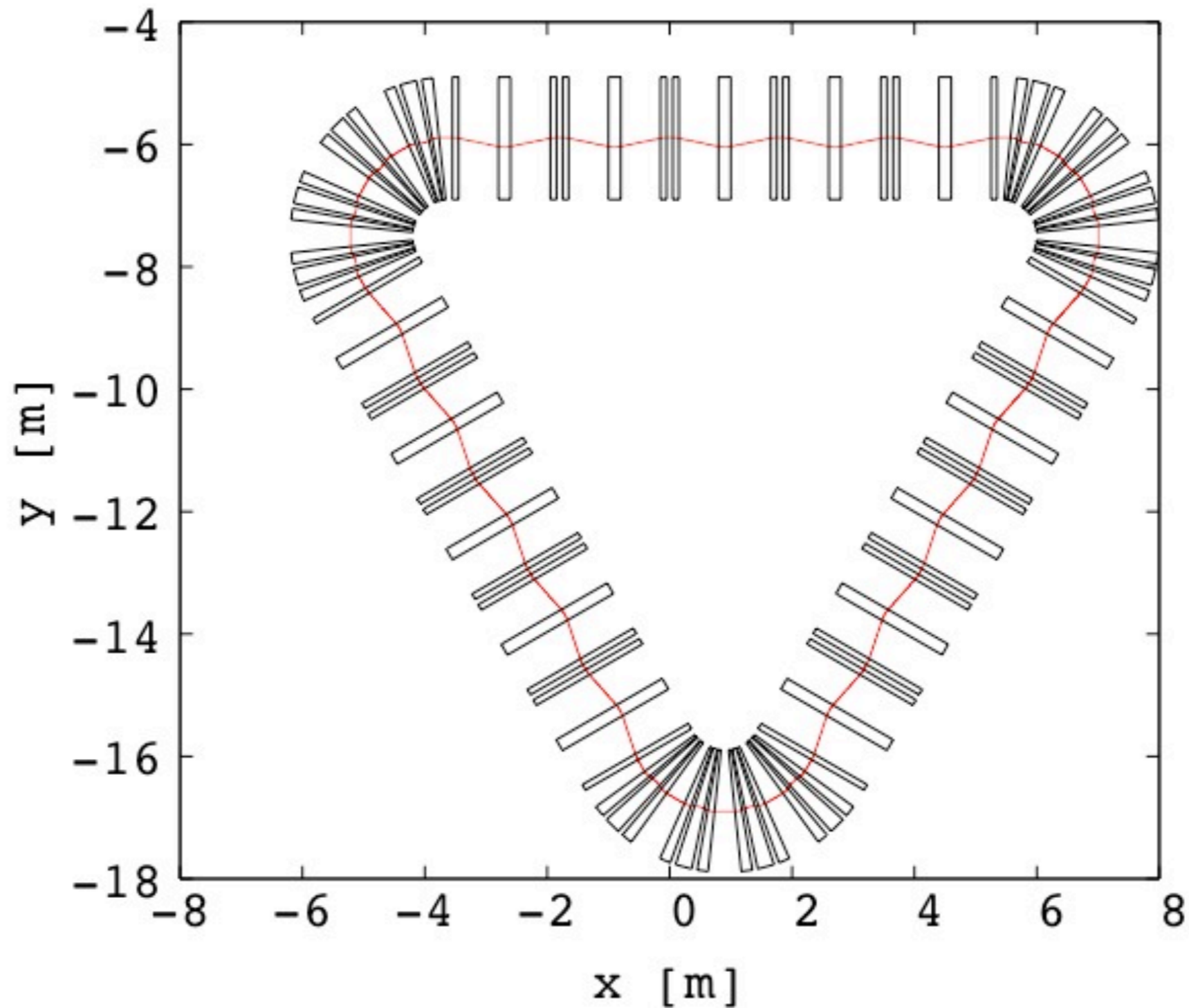
Applications

Betafunctions (half ring) of race-track PRISM



Applications

Another solution?



Summary

- Scaling FFAG lattices have intrinsic good features (fixed field magnets, large acceptance, possibility of using constant RF cavities) for muon acceleration.
- New tools have been recently developed to introduce more flexibility of the scaling FFAG for muon acceleration.
- This is only the start!

Thank you for your attention

Simulation tools

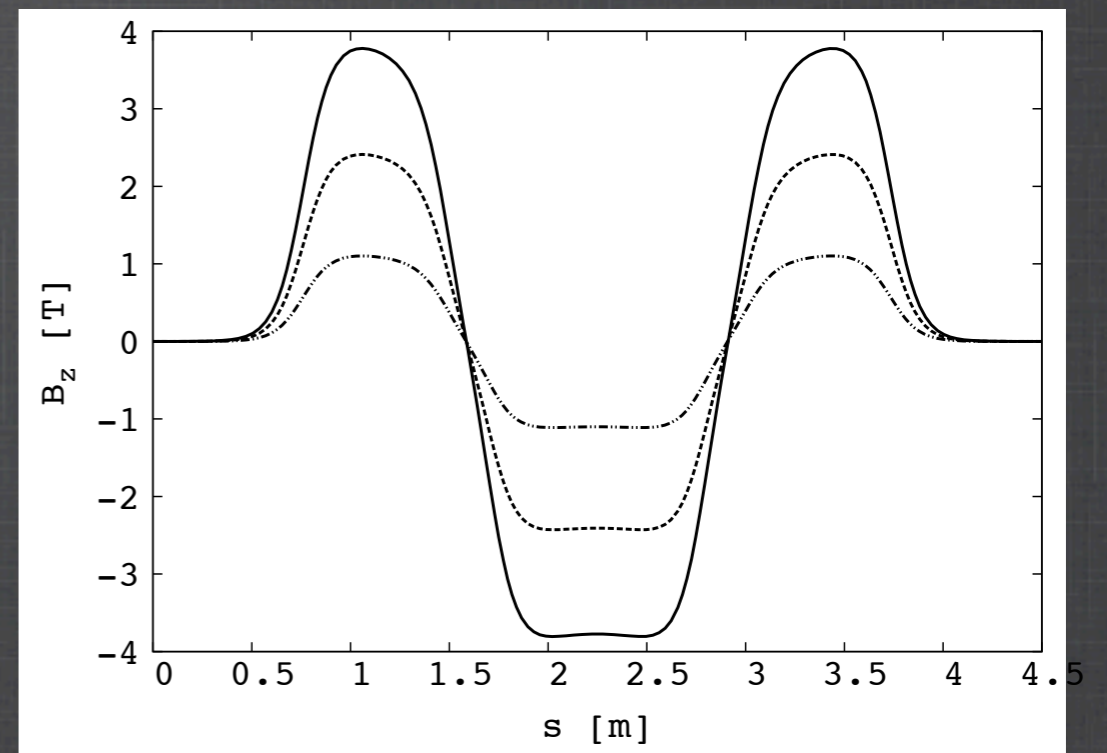
Step-wise particle tracking in geometrical field models

- Two codes:
 - KUT-code,
 - + benchmark using Zgoubi.

- Mid-plane field distribution follows:

$$B(r, \theta) = B_0 \left(\frac{r}{r_0} \right)^k \mathcal{F}(\theta).$$

- Enge type of field fall-off.
- Field off the mid-plane is obtained, from a 4th order expansion (following Maxwell's equations).



Vertical component of the magnetic field along the closed orbits at 3.6 GeV (dot-dashed line), 8.0 GeV (dotted line) and 12.6 GeV (solid line).